Developmental pathways underlying sexual differentiation in a U/V sex chromosome system

Daniel Liesner[1*], Guillaume Cossard[1], Min Zheng[1], Olivier Godfroy[2], Josué Barrera-Redondo[1], Fabian B. Haas[1], Susana M. Coelho[1*]

[1]Department of Algal Development and Evolution, Max Planck Institute for Biology Tübingen, Max-Planck-Ring 5, 72076 Tübingen, Germany

[2]Station Biologique de Roscoff CNRS, Sorbonne Université, France

[*]Correspondence: susana.coelho@tuebingen.mpg.de; daniel.liesner@tuebingen.mpg.de

Abstract

In many multicellular organisms, male and female developmental fates are not determined by the classic XX/XY or ZW/ZZ systems but rather by a third type of sex chromosomes, the U/V sex chromosomes. In U/V systems, sex is expressed in the haploid phase, with U chromosomes confined to females and V chromosomes to males. Here, we explore several male, female and partially sex-reversed male lines of a giant kelp with a U/V system, to decipher the role of U/V sex chromosomes and autosomes in the initiation of male versus female developmental programs. Using comparative transcriptomics and experimental approaches, we identify a small set of genes located on the V- and U sex chromosomes that play a role in triggering the male versus female developmental programs, and we uncover a subset of autosomal effector genes. We describe the transcriptomic pathways underlying sexual differentiation and show that male, but not female, developmental fate involves large-scale transcriptome reorganization with pervasive enrichment in regulatory genes affecting the expression of more than half of the giant kelp genome. Furthermore, male-biased genes are more species-specific and exhibit faster evolutionary rates than unbiased genes, whereas genes underlying female developmental fate are more evolutionary conserved. Our observations imply that a female-like phenotype is the "ground state" of the giant kelp morphology, which is complemented by the presence of a U-chromosome, but overridden by a dominant male developmental program in the presence of a V-chromosome.

Introduction

Morphological sexual dimorphism occurs at different levels in most species with separate sexes, which consist of most animals and some plants[1,2]. Classically, asymmetry in gamete size is used as the defining characteristic of a male versus a female, and is the starting point of sexual dimorphism[3]. Assuming that zygote size correlates with survival[1], disruptive selection leads to the evolution of different gamete sizes[4]. This in turn drives the selection of sex-specific traits to accommodate for increased provisioning in individuals producing large gametes (*i.e.*, females) and sexual competition in those producing small gametes (*i.e.*, males)[2,3]. The establishment of the male versus female developmental programs depends often on a specific genomic region which is different between males and females, *i.e.*, a sex determining region (SDR) located on sex chromosomes[5,6]. Gene(s) present in this region trigger the differential expression of a downstream cascade of autosomal effector genetic pathways, eventually leading to sex-biased gene expression[7,8]. Sex determination and sexual differentiation have been extensively studied in animals and plants, often by genomic and transcriptomic comparison between sexes (see, *e.g.*, reviews by Charlesworth[9]; Feng et al.[10]) but also using sex-reversed mutants[11–14]. Beyond the causal mutation which often highlights key sex determining genes, the transcriptomic restructuring of autosomal gene expression in these mutants is expected to shed light on the core molecular pathways involved in sexual phenotype differentiation[15,16]. However, in other groups of multicellular eukaryotes besides animals and some plants, knowledge on the key genes involved in sex phenotype differentiation remains elusive[17,18].

Brown algae are one of few eukaryotic lineages to have independently evolved complex multicellularity, defined as a macroscopic body plan consisting of multiple cell types that is constructed by developmental programs involving cell division and differentiation[19]. This group of ecologically keystone organisms present a wide range of sexual systems and levels of sexual differentiation[20]. Most brown algae are dioicous, *i.e.*, male and female sexes are present in separate individuals and are determined in the haploid (gametophyte) stage[21]. Haploid genetic sex determination operates *via* a U/V sexual system, in which females possess a U chromosome and males a V chromosome[22]. Sexual dimorphism of gametophytes is driven by sex-biased expression of autosomal genes[23] and is thought to involve effector genes operating downstream of master regulator(s) located on the sex-determining regions (SDR) of the U and V sex chromosomes[22,24]. Across several brown algae, the master male-determining gene (male inducer, *MIN*)[25] located on the V-SDR encodes a HMG-box protein[22,24–28].

The filamentous gametophytes of the brown algal order Laminariales (*i.e.*, kelps) are oogamous (*i.e.*, female gametophytes produce large eggs and male gametophytes produce small sperm cells) and present a relatively simple sexual dimorphism[29]. Female gametophyte cells are larger, contain larger chloroplasts[29], and upon gametogenesis develop into oogonia (**Figure 1A**). One immotile egg cell is released and remains attached to the oogonium[30]. Male gametophytes, in contrast, consist of smaller, less pigmented cells, which produce sperm by mitosis in antheridia. Note that males produce high quantities of sperm whereas females produce small quantities of eggs [31]. Sperm release and attraction is facilitated by the pheromone lamoxirene which is produced by the eggs[32]. Syngamy and embryo development leads to the diploid sporophyte generation, which may grow to tens of meters in length (**Figure 1A**). Unfertilized eggs may also develop parthenogenetically into partheno-sporophytes which are often deformed and not viable[33,34]. In mature sporophytes, meiosporangia are arranged in distinct sori, which in some species develop on specialized blades called sporophylls, and release haploid meiospores, which settle and germinate into initial gametophyte cells (**Figure 1A**).

Recently, a genetically male gametophyte with a partially sex-reversed phenotype has been described in the giant kelp *Macrocystis pyrifera*[24]. Male gametophytes of this variant line exhibited an increased cell size and produced immotile gametes which were capable of parthenogenesis. However, these egg-like gametes did not produce the sperm-attracting pheromone lamoxirene[24] and were therefore sterile. The sterility of the line precluded a detailed genetic analysis of the causative and effector genes underlying this phenotype.

Here, we exploit two additional giant kelp individuals that are genetically male but present feminisation phenotypes, to examine the core molecular processes underlying sexual dimorphism in a haploid U/V sexual system. The availability of these independently-obtained feminised individuals, together with closely related male and female wild type (WT) lines, allowed us to estimate the extent of the conservation of the molecular events underlying the male versus female developmental program, in particular to disentangle the role of sex-linked genes and autosomal gene expression in the initiation of sex-specific development, and also to examine the conservation of the gene regulatory networks that underlie sexual dimorphism in these organisms. We use experimental approaches to show that all three independently obtained feminised lines share similarly feminised developmental patterns, which are accompanied by feminisation and de-masculinisation of gene expression. We examine the transcriptomes and reveal that effector genes related to central metabolic pathways are consistently associated with feminisation, as well as a subset of genes located on the sex chromosomes. Finally, we show that male development involves large-scale restructuring of gene expression patterns and propose that a female-like phenotype is the "ground state" of the giant kelp morphology, which is complemented by the presence of a U-chromosome, but overridden by a dominant male developmental program in the presence of a V-chromosome.

Results

Identification of genetically male lines showing feminised developmental patterns

We had previously reported the identification of the giant kelp line Mpyr_13-4, which presented a feminised phenotype morphology and a range of female features, despite being genetically male[24]. This feminised variant originated from a male gametophyte collected in Curahue (Cur), Chile, following treatment with colchicine (**Figure S1**). This line, however, was sterile, precluding more exhaustive genetic studies to understand the molecular basis of the phenotype. We reasoned that comparing independently obtained male lines with a similarly feminised phenotype should allow to study the extent of conservation of the pathways involved in sexual differentiation and also to pinpoint crucial genes required for male and female developmental functions. We therefore examined a collection of wild type (WT) and variant *M. pyrifera* strains from another population (Curaco de Vélez, Chile; CVe) that had been subjected to the same colchicine treatment independently, to identify further strains presenting a similar feminisation phenotype.

Our screen identified two additional genetically male lines exhibiting a feminised phenotype, Mpyr_fem1 and Mpyr_fem2 (**Figure 1**; **Figure S1**). We used PCR markers (**Table S1**) to confirm that these lines were *bona fide* genetically males (*i.e.*, had only the V and not the U-sex chromosome; **Figure S2**). Flow cytometry analysis of DNA content provided no evidence for large-scale chromosome doubling compared to WT male samples (**Figure S3**), indicating that the colchicine treatment had not induced aneuploidy. Therefore, Mpyr_fem1 and Mpyr_fem2 represent two independently feminised lines, in addition to Mpyr_13-4[24].

We performed a detailed morphometric analysis to characterize the phenotype of these two variant lines compared with WT male and female lines (**Figure 1**). Gametophyte cells of both variants were of intermediate size compared to the WT male and female lines (**Figure 1B**). Cell size differed significantly between lines (**Figure 1B**; Kruskal-Wallis $X^2 = 283.64$, df = 3, $p < 0.0001$), with variant cells being significantly smaller than WT female cells (pairwise Wilcoxon test, $p < 0.0001$) and significantly larger than WT male cells (pairwise Wilcoxon test, $p < 0.0001$).

During induction of gametogenesis (see methods), gametophyte cells of both variant lines developed into elongated gametangia, which resembled female oogonia (**Figure 1D-F**). From these, large, immotile gametes were released (**Figure 1F-G**). Gamete size differed significantly between lines (**Figure 1C**; Kruskal-Wallis $X^2 = 319.51$, df = 3, $p < 0.0001$), with variant gametes (**Figure 1F-G**) being significantly larger than WT male gametes (**Figure 1H**; pairwise Wilcoxon test, $p < 0.0001$), but significantly smaller than WT female gametes (**Figure 1I**; pairwise Wilcoxon test, $p < 0.0001$).

In *M. pyrifera*, only female gametes may undergo parthenogenesis if they are not fertilized by male gametes (**Figure 1L**), leading to development of partheno-sporophytes that morphologically resemble diploid sporophytes[33,35]. We observed development of partheno-sporophytes from unfertilized gametes in both genetically male variants (**Figure 1J-K**).

WT eggs of *M. pyrifera* release the pheromone lamoxirene which induces the release of male gametes from neighbouring male gametophytes. Male gametes, attracted by the chemical cue, actively swim towards the eggs and syngamy occurs (see **Figure 1A**). We next tested whether the egg-like structures produced by the feminised males were functional eggs, *i.e.*, whether they were capable of attracting male gametes. When we brought fertile male gametophytes in contact with a wild type female strain, sperm was immediately released, attraction and gamete fusion occurred (**Figure 1M**), and sporophytes developed within few days (**Figure 1N**). In strike contrast, when introducing fertile WT male gametophytes to the cultures of the Mpyr_fem1 and Mpyr_fem2 variants, no sperm was released and no gamete fusion occurred. These observations suggest that, similarly to the variant Mpyr_13-4 described previously[24], our two additional feminised lines Mpyr_fem1 and Mpyr_fem2 are also incapable of attracting and fusing with males, suggesting the egg-like gametes do not produce lamoxirene and are therefore not fully functional eggs.

Together, these results suggest that although the two variant lines share morphological features with females (*e.g.*, larger cell dimensions, gamete morphology, parthenogenetic capacity), they are only partially sex-reversed, *i.e.*, they are not fully functional females.

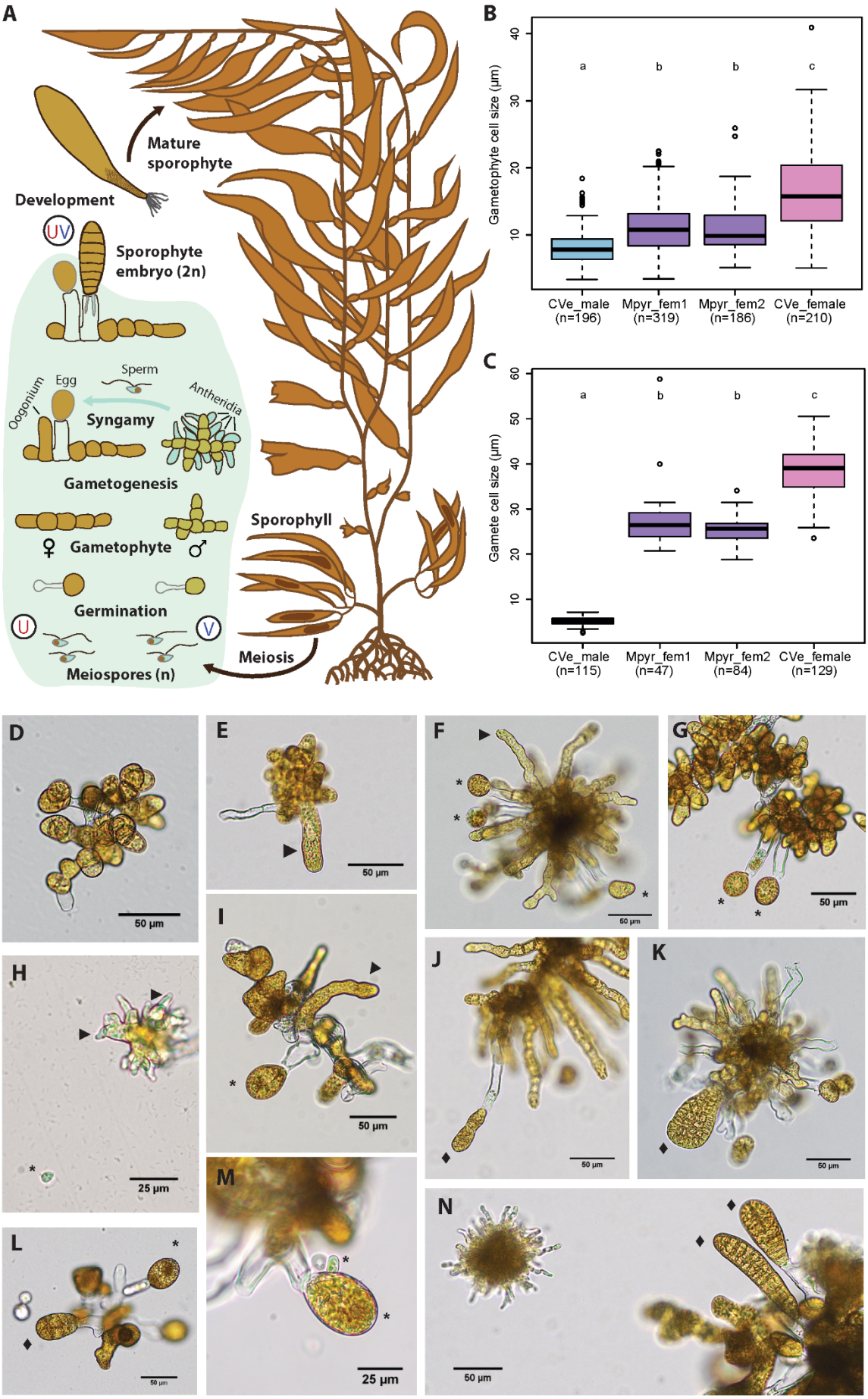
A
Mature sporophyte
Development
UV
Sporophyte embryo (2n)
Sperm
Egg
Oogonium
Antheridia
Syngamy
Gametogenesis
Sporophyll
♀ Gametophyte ♂
Germination
U
V
Meiospores (n)
Meiosis
B
Gametophyte cell size (µm)
a
b
b
c
CVe_male (n=196)
Mpyr_fem1 (n=319)
Mpyr_fem2 (n=186)
CVe_female (n=210)
C
Gamete cell size (µm)
a
b
b
c
CVe_male (n=115)
Mpyr_fem1 (n=47)
Mpyr_fem2 (n=84)
CVe_female (n=129)
D
E
F
G
H
I
J
K
L
M
N
50 µm
25 µm

Figure 1 Morphology and observations of *Macrocystis pyrifera* WT male (CVe_male) and female (CVe_female) gametophytes, and the feminised male gametophytes Mpyr_fem1 and Mpyr_fem2. (**A**) Schematic life cycle of *M. pyrifera*, with microscopic, haploid stages highlighted in light green. Mature sporophytes (2n) release meiospores (n) from sori located on sporophylls. Meiospores settle and germinate into distinct, microscopic female and male gametophytes, which carry the U and V chromosome, respectively. Following gametogenesis, females release eggs from oogonia, which release the pheromone lamoxirene. This triggers the release and attraction of spermatozoids from male antheridia. Syngamy initiates the next sporophyte generation. (**B**) Gametophyte cell size of WT male and female gametophytes and the feminised males. Letters above plot indicate significant differences between strains (pairwise Wilcoxon test, $p < 0.0001$). (**C**) Gamete cell size of WT male and female gametophytes and the feminised males. Letters indicate significant differences between strains (pairwise Wilcoxon test, $p < 0.0001$). (**D**) Vegetative Mpyr_fem2 gametophyte. (**E**) Mpyr_fem1 gametophyte with gametangium (arrow). (**F**) Mpyr_fem2 with gametangium (arrow) and released gametes (asterisks). (**G**) Mpyr_fem1 gametophyte with released gametes (asterisks). (**H**) Fertile wild type male gametophyte with antheridia (arrows) and spermatozoid (asterisk). (**I**) Fertile wild type female with oogonium (arrow) and released eggs (asterisk). (**J**) Mpyr_fem1 gametophyte with partheno-sporophyte (diamond). (**K**) Mpyr_fem2 gametophyte with partheno-sporophyte (diamond). (**L**) Wild type female gametophyte with partheno-sporophyte (diamond). (**M**) Fusion of male and female gametes (asterisks). (**N**) Sporophytes obtained from syngamy (diamonds) in co-cultivation of male and female gametophytes.

Feminisation and de-masculinisation of gene expression underlie the phenotype of Mpyr-fem1 and Mpyr-fem2

In order to investigate the molecular pathways associated with the morphological feminisation of the variant lines, we used an RNA-seq approach using triplicate samples from the variants Mpyr_fem1 and Mpyr_fem2 in comparison to the WT male from which they were derived and to a WT female from the same population (CVe; **Table S2**; **Figure S1**). In our analysis, we also included the similarly feminised line Mpyr_13-4, which was independently obtained from a male of a different natural population (Cur)[24], using publicly available datasets (**Table S2**).

Hierarchical clustering based on z-scores calculated from normalized expression values (transcripts per million, TPM) for all 22,186 annotated genes confirmed similarity among replicates of the same strain (**Figure S4**). The global gene expression patterns of the two feminised CVe variants Mpyr_fem1 and Mpyr_fem2 clustered intermediately to the respective WT males and females (**Figure S4A**). Mpyr_fem1 and Mpyr_fem2 formed a distinct cluster, which shared a node with the WT male CVe30m from which they arose. We noticed that the feminised variant Mpyr_13-4 clustered more closely with the WT female Cur4f than with the WT male Cur6m (**Figure S4B**). This result opens the possibility that there may be different degrees of "feminisation" of the variant strains, with Mpyr_13-4 being more strongly feminised compared to Mpyr_fem1 and Mpyr_fem2.

In order to further investigate the feminised transcriptomic pattern of the variants, we focused on genes that are differentially expressed between males and females (sex-biased genes, SBG) and how they change during the feminisation process. We treated each population separately, *i.e.*, we extracted separate sets of SBGs within each the CVe and Cur population based on the comparisons of WT males and WT females using DESeq2[36].

For the CVe population, we found 1,375 male-biased genes (MBGs) and 1,631 female-biased genes (FBGs; **Table S3**). For the Cur population we found 2,287 MBGs and 2,387 FBGs (**Table S4**). The proportion of SBG was significantly higher in Cur than in CVe for both MBG (Cur: 12.72%; CVe: 8.18%; test of equal proportions; $X^2 = 189.68$, $p < 2.2*10^{-16}$) and FBG (Cur: 13.06%; CVe: 9.57%; $X^2 = 106.75$, $p < 2.2*10^{-16}$). The fraction of FBGs was significantly higher than that of MBGs in the CVe population ($X^2 = 20.17$, $p = 7.1*10^{-6}$), but not in the Cur population ($X^2 = 0.98$, $p = 0.3225$). The two populations shared 682 FBGs and 489 MBGs (**Figure S5**) so only 24.1% of all FBGs and 16.2% of all MBGs are consistently sex biased in the same sex in both populations. Together, our observations suggest there is a relatively high turn-over in terms of SBG expression between these populations. Interestingly, we noticed that

the fraction of shared FBGs was significantly higher than that of shared MBGs (test of equal proportions; $X^2 = 27.91$, $p = 1.27*10^{-7}$), *i.e.*, MBGs appear to show a higher turnover between the two populations compared to FBGs. This trend was confirmed by examining the turn-over of sex bias across larger phylogenetic distances (**Figure 2**), using published datasets from four other brown algal species with separate sexes[37]. We found 1,126 single-copy orthogroups across all species (**Table S5**). Among these, there were highly significant overlaps (multi-set interaction analysis[38]) of female-biased orthologs of (at least one population of) *M. pyrifera* which were also female-biased in the other species (**Figure 2A**). In stark contrast, no MBGs of *M. pyrifera* were orthologous to all four other species (**Figure 2B**). In addition, while both FBGs and MBGs have accumulated significantly more synonymous substitutions (dS) than unbiased genes (**Figure 2C**; orthologous genes between *M. pyrifera* and *Saccharina japonica*; Wilcoxon test, $p = 1.28x10^{-6}$, $p = 9.23x10^{-6}$, respectively), the ratio of nonsynonymous over synonymous substitutions (dN/dS) was significantly lower in FBGs compared to unbiased genes (**Figure 2D**; $p = 2.57x10^{-9}$), and significantly higher in MBGs ($p = 4x10^{-26}$). Therefore, it appears that MBGs are more species-specific and present faster evolutionary rates than FBGs.

We then compared the expression of SBGs in WT males, WT females and variants. A clear trend of transcriptome feminisation and de-masculinisation emerged in the variants when comparing differentially expressed genes (DEGs) in the variant to the SBGs within their respective populations (**Figure 2E-F**). The majority of significantly up-regulated genes in the variants was also female-biased in the same population (multi-set intersection analysis, $p < 0.0001$ for all; **Figure 2E**), and the majority of significantly down-regulated genes in the variants was male-biased (multi-set intersection analysis, $p < 0.0001$ for all; **Figure 2F**). Considering the global expression of all SBGs [as log(TPM+1)], the expression levels of FBGs were significantly higher in the variants than in the males (Wilcoxon test; Mpyr_13-4 and Mpyr_fem2, $p < 0.0001$; Mpyr_fem1, $p < 0.001$), but significantly lower than those of WT females (Wilcoxon test; Mpyr_fem1 and Mpyr_fem2, $p < 0.0001$; Mpyr_13-4, $p < 0.001$; **Figure 2G**). Comparably, the mean expression level of male-biased genes in the variants was significantly lower in the variants than in the males (Wilcoxon test; $p < 0.0001$ for all variants), but still significantly higher than in females (Wilcoxon test; $p < 0.0001$ for all variants; **Figure 2H**). Therefore, the partially sex-reversed phenotype of the variants co-occurs with significant feminisation and de-masculinisation of global gene expression patterns.

We further compared the magnitude of differential expression (as log_2 fold-change, log_2FC) for DEGs in several comparisons of variant vs. WT male (*i.e.*, co-DEGs for these comparisons). For instance, 345 genes are co-DEGs between the comparisons Mpyr_fem1 vs. CVe30m and Mpyr_13-4 vs. Cur6m, and 510 genes are co-DEGs between the comparisons Mpyr_fem2 vs. CVe30m and Mpyr_13-4 vs. Cur6m. A highly significant correlation of log_2FC within each of these set of co-DEGs (**Figure S6A,B**; R = 0.66, $p < 0.0001$; R = 0.64, $p < 0.0001$, respectively) indicates that a core set of genes is expressed at comparable levels during feminisation across independent experiments. Between Mpyr_fem1 and Mpyr_fem2, the correlation of the 484 co-DEGs is very close to one (**Figure S6C**; R = 0.97, $p < 0.0001$). Together, these results show that, despite the high turnover of SBG expression across populations, all variants converge to similar patterns of transcriptome feminisation and de-masculinisation, which involve a central set of genes that undergoes similar changes in expression patterns across independent experiments.

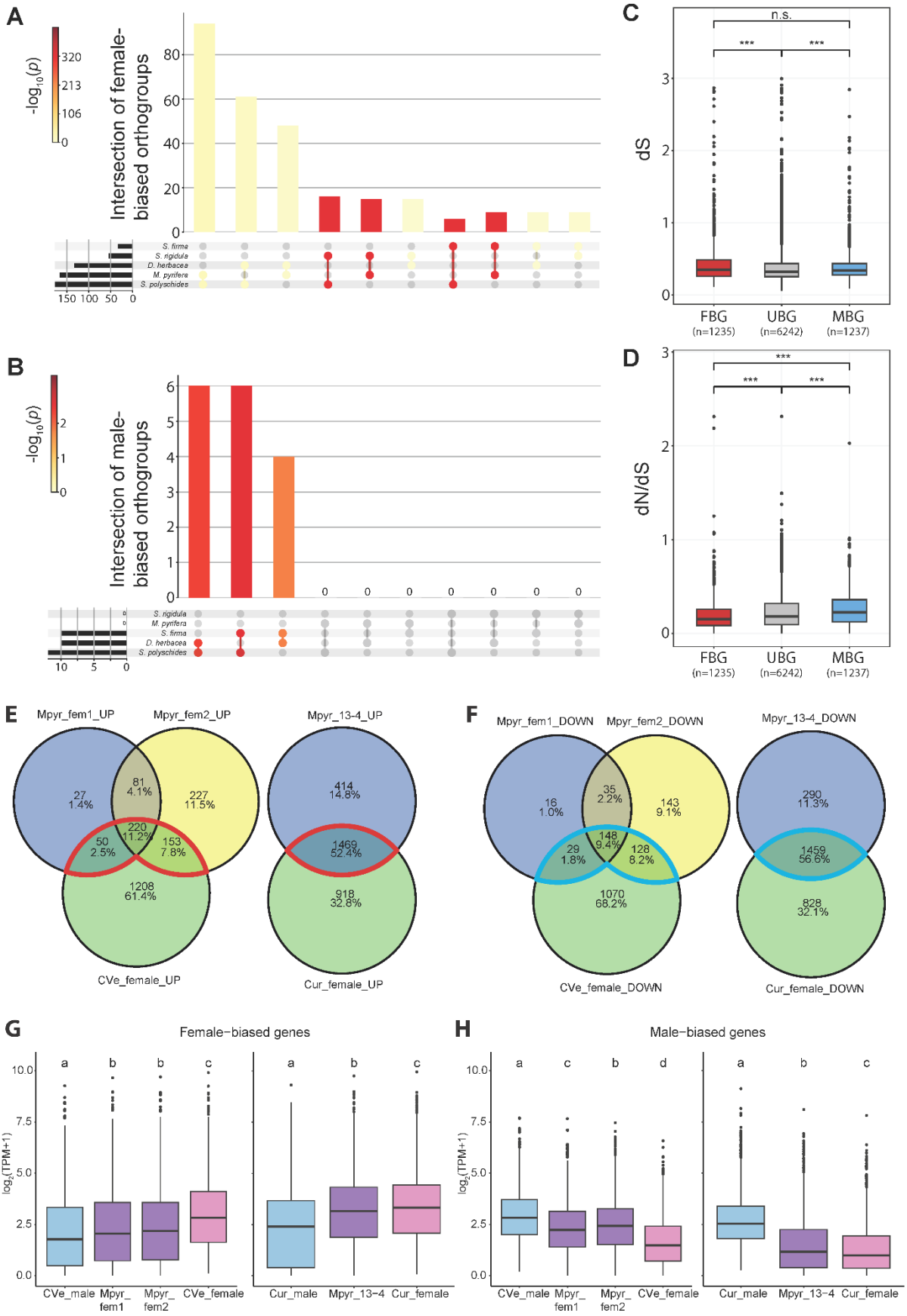
A
-log10(p)
320
213
106
0
Intersection of female-biased orthogroups
80
60
40
20
0
S. firma
S. rigidula
D. herbacea
M. pyrifera
S. polyschides
150 100 50 0
B
-log10(p)
2
1
0
Intersection of male-biased orthogroups
6
5
4
3
2
1
0
S. rigidula
M. pyrifera
S. firma
D. herbacea
S. polyschides
10 5 0
C
n.s.
***
***
dS
FBG (n=1235)
UBG (n=6242)
MBG (n=1237)
D
***
***
***
dN/dS
FBG (n=1235)
UBG (n=6242)
MBG (n=1237)
E
Mpyr_fem1_UP
Mpyr_fem2_UP
Mpyr_13-4_UP
27 1.4%
81 4.1%
227 11.5%
414 14.8%
220 11.2%
50 2.5%
153 7.8%
1469 52.4%
1208 61.4%
918 32.8%
CVe_female_UP
Cur_female_UP
F
Mpyr_fem1_DOWN
Mpyr_fem2_DOWN
Mpyr_13-4_DOWN
16 1.0%
35 2.2%
143 9.1%
290 11.3%
148 9.4%
29 1.8%
128 8.2%
1459 56.6%
1070 68.2%
828 32.1%
CVe_female_DOWN
Cur_female_DOWN
G
Female-biased genes
log2(TPM+1)
10.0
7.5
5.0
2.5
0.0
a b b c
a b c
CVe_male
Mpyr_fem1
Mpyr_fem2
CVe_female
Cur_male
Mpyr_13-4
Cur_female
H
Male-biased genes
log2(TPM+1)
10.0
7.5
5.0
2.5
0.0
a c b d
a b c
CVe_male
Mpyr_fem1
Mpyr_fem2
CVe_female
Cur_male
Mpyr_13-4
Cur_female

Figure 2 Sex-biased gene expression of *Macrocystis pyrifera* gametophytes. **(A,B)** Intersection plots showing the occurrence of sex-biased orthologs among the five brown algae species *Desmarestia herbacea*, *M. pyrifera*, *Saccorhiza polyschides*, *Sphacelaria rigidula*, and *Sphaerotrichia firma*, based on female-biased genes **(A)** and male-biased genes **(B)** in *M. pyrifera* (considering sex bias in at least one *M. pyrifera* population); *p*-values are obtained by intersection analysis (SuperExactTest). **(C,D)** Sequence divergence measured as synonymous substitution rate **(C)** and ratio of non-synonymous over synonymous substitutions **(D)** of sex-biased (FBG, female-biased genes; MBG, male-biased genes) and unbiased genes (UBG) that are orthologous between *M. pyrifera* and *Saccharina japonica* (***, $p < 0.001$; Wilcoxon test). **(E-F)** Venn diagrams depicting the absolute number and fraction of significantly up-regulated **(E)** and down-regulated **(F)** genes within the *Macrocystis pyrifera* populations CVe (Mpyr_fem) and Cur (Mpyr_13-4). Subsets associated with feminisation (up-regulated female-biased genes) and de-masculinisation (down-regulated MBG) are highlighted in red and blue, respectively (DESeq2, $n = 3$ for CVe; $n = 2$ for Cur). **(G,H)** Transcript abundance of FB (**G**) and MB (**H**) genes in *Macrocystis pyrifera* male WT (CVe_male, Cur_male), feminised male variants (Mpyr_fem1, Mpyr_fem2, Mpyr_13-4) and female WT (CVe_female, Cur_female). Letters denote statistical differences between strains (Kruskal-Wallis test, pairwise Wilcoxon rank sum test, $p < 0.05$).

Functional categorization of effector genes involved in feminisation and de-masculinisation

To identify the potential functional gene categories involved in the feminised phenotype of the variants, we explored enriched gene ontology (GO) terms among gene sets related to feminisation and de-masculinisation. We extracted the FBGs that were up-regulated in the variants (**Figure 2E-F**) reasoning that these genes are important for the phenotype. We then identified GO terms which were significantly enriched in all three sex-biased subsets of variant DEGs (**Figure 3**). Among these, we explored the individual functional gene annotations to infer the affected pathways more specifically. This approach revealed several shared GO terms associated with feminisation that had predicted functions related to polysaccharide metabolism (**Figure 3A-B**; **Table S6**), and likely involve cell wall alginate synthesis. In combination with the up-regulation of the "polysaccharide catabolic process" category these results strongly indicate a distinct cell wall composition in females and feminised males compared to WT males. Functions related to signalling processes were consistently differentially expressed. For instance, "calmodulin binding" was up-regulated (**Figure 3B**), while transmembrane receptor kinases related to the phosphorelay signal transduction system were down-regulated in the feminised variants (**Figure 3C**; **Table S7**), as were leucine rich repeat calcium binding proteins (**Figure 3D; Table S7**). While the biological process "cell cycle checkpoint signalling" is down-regulated (**Figure 3C; Table S7**) and consists mainly of serine/threonine kinases and one cyclin D3 annotation, "regulation of cell growth" is up-regulated (**Figure 3A**; **Table S6**), and several genes with ankyrin repeat motifs related to "mitotic cytokinesis" are both up- and down-regulated (**Figure 3A,C**; **Table S6,S7**).

In summary, core shared effector gene functions associated with feminisation and de-masculinisation suggest that protein signalling is central to sexual differentiation in brown algae, and that polysaccharide and cell wall metabolism play a key role in the distinct sexual program of development of these organisms.

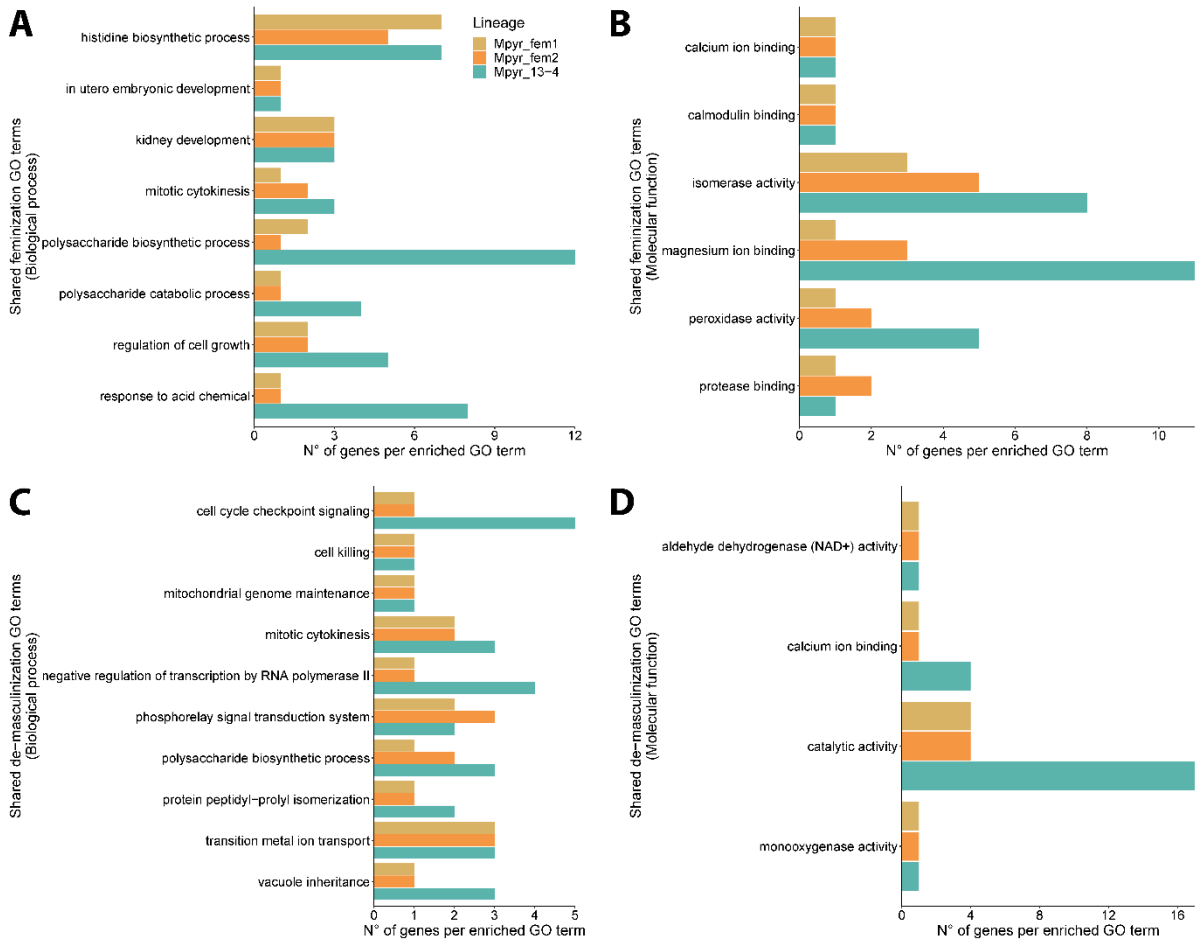

Figure 3 Number of genes within each significantly enriched gene ontology (GO) term shared by all within-population comparisons of feminised males and females vs. WT males of *Macrocystis pyrifera*, representing conserved effector gene functions of feminisation **(A,B)** and de-masculinisation **(C,D)** in the GO categories of biological process **(A,C)** and molecular function **(B,D)**.

Genes located on the sex chromosome may play a key role in feminisation

We examined the changes in expression of genes located on the V chromosome of *M. pyrifera* during feminisation. Among seven previously identified ancestral male-linked genes[26], three showed a consistently reduced transcript abundance across the variants (**Figure 4**). Two genes had been identified previously in Mpyr_13-4[24]: the male-master determining gene Mp_HMG (male inducer *MIN*)[22,25], and Mp_13-001840, a transmembrane protein with potential receptor functions (**Figure 4C**). In addition, both variants Mpyr_fem1 and Mpyr_fem2 show significant down-regulation of Mp_13-001410, which encodes a protein with a WD40/YVTN repeat-like-containing domain. In order to examine sequence variation on coding sequences of SDR genes in the variant strains compared to male WT strains, we used RNA-seq read mapping data for sequence variant calling. Ten potential candidate loci in the CVe population and seven candidate loci in the Cur population were found and curated manually in the genome browser JBrowse[39]. We identified all reported mutations as false positives due to differences in variant calling based on read coverage (**Figure S7**). Therefore, we conclude that the reduced transcript abundance of SDR genes was not the result of mutations in the coding sequence of these genes.

Our dataset comparison further allowed us to estimate the number and identity of the genes that are exclusively expressed in fully functional WT females, presumably constituting the key gene set that is crucial for the establishment of a functional female program. We found 785 genes which were exclusively expressed (TPM > 5th percentile) in WT female CVe13f and 429 genes which were exclusively expressed in the WT female Cur4f (**Table S8**). Of these, 98 genes were shared between both female WT, and 24 of these were additionally DEGs with significantly higher expression in both females compared to the respective within-population genetically male strains, including the variants (**Table S8**). We therefore consider these 24 genes to be the "core" female-restricted gene set. This gene set was enriched in putative functions related to GO terms "nucleotide binding", "nucleic acid binding", and "DNA binding" (**Table S9**).

Remarkably, more than half (14 out of 24) of these are genes located on the sex chromosome of *M. pyrifera* (scaffold_2 in female reference genome by Diesel et al.[40]; **Table S10**). Additionally, seven of these have orthologs on the sex chromosome of *Ectocarpus* (including two genes shown to be sex-linked in *M. pyrifera*[26]). Gene g33225 has strong sequence homology to *Ectocarpus* gene Ec-sdr_f_000170 which is a conserved female sex-linked gene across brown algae taxa, in which case it is likely a gametolog to Mp_13-001840 described above[26,28]. Similarly, the ortholog of gene g35582 is the conserved female-linked *Ectocarpus* gene Ec-sdr_f_000010 and is likely a gametologue to the male-linked Mp_13-001910. Together, these analyses indicate that multiple genes located on the sex chromosome may operate in concert with autosomal genes to initiate and maintain sexually dimorphic developmental programs in the giant kelp.

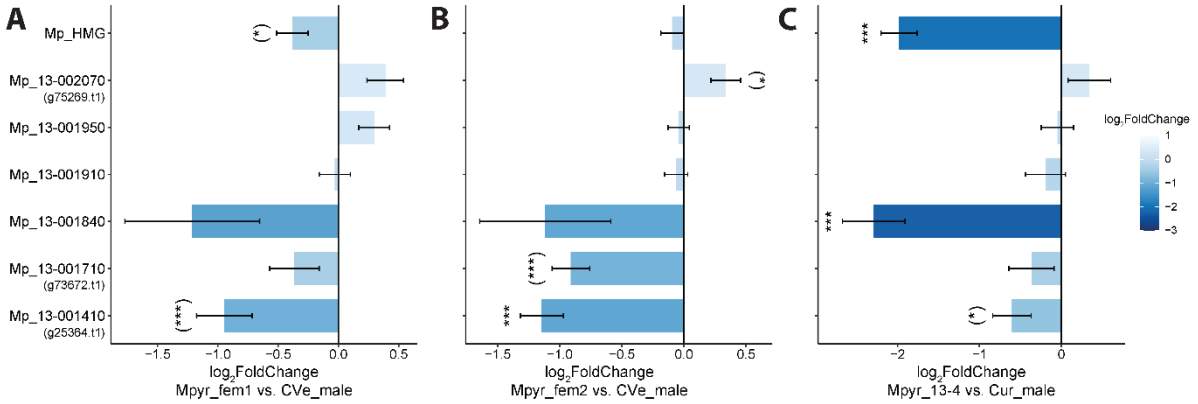

Figure 4 Differential expression of *Macrocystis pyrifera* sex-linked genes for each feminised variant vs. wild type male (mean values ± SE, DESeq2, n=3 for **A,B**; n=2 for **C**). Genes are named according to their *Ectocarpus* orthologs (as in Müller et al.[24]); note that gene names for Mp_13-001410, Mp_13-001710 and Mp_13-002070 are g25364, g73672 and g75269, respectively, in the genome annotation[42]. Asterisks indicate significance of differential expression (*, $p < 0.05$; ***, $p < 0.001$), and are reported in parentheses if the expression magnitude threshold of $|\log_2\text{FoldChange}| > 1$ is not met.

Enrichment of regulatory genes underlies male-specific development

In addition to the differential gene expression analysis, we also performed a weighted gene co-expression network analysis (WGCNA)[43] to identify modules of co-regulated genes and to relate these to the male and female developmental patterns across all samples simultaneously. We assigned four traits to each replicate sample (**Figure S8**): mean gametophyte cell size (see **Figure 1B**), mean gamete cell size (see **Figure 1C**), genetic sex (1 = U-chromosome, 0 = V-chromosome), and parthenogenesis (1=present, 0=absent). After removing genes with null expression, we clustered 20,054 genes into 39

modules with a minimum size of 30 genes per module, which are named after colours by default (**Figure 5**). Size of the modules ranged from 33 genes in module magenta4 to 5,075 genes in module blue.

We identified twelve modules related to sex phenotype differentiation, which showed a significant Pearson's correlation ($|R| \geq 0.6$; $p \leq 0.01$) to at least one trait (highlighted in bold font in **Figure 5**). Of these, six modules were negatively correlated with female traits (blue, coral2, navajowhite2, plum, firebrick4, darkorange) and six modules were positively correlated with female traits (greenyellow, plum1, skyblue1, lightsteelblue, magenta, green). Accordingly, most of these modules were significantly enriched (multi-set intersection analysis) with genes that we had previously identified as sex-biased (**Figure 5**; **Tables S11-S12**). Notably, the three largest modules, blue, coral2 and darkorange, were strongly negatively correlated to traits associated with feminisation, and, accordingly, were significantly enriched in male-biased genes (multi-set intersection analysis, $p < 0.0001$; **Figure 5**). The six modules related to male traits consisted of in total 12013 genes (54.15% of the whole transcriptome), whereas the six female trait-related modules consisted of 4163 genes (18.76%).

GO term enrichment analysis of these twelve modules confirmed the widespread involvement of signal transduction in the regulation of sexual differentiation and the responses of polysaccharide metabolism which is affected across sex phenotypes (see above; **Figure S9**). The enrichment of mitosis- and cell cycle-related GO terms in the male trait-biased modules is notable, consistent with strong mitotic activity related to sperm production, as well as the significant enrichment of cilium movement in the male-biased module darkorange. Enrichment in functions related to chromatin structure and epigenetic histone marks suggests that they are key components in processes underlying male development (**Figure S10**). In addition, the enrichment of functions related to DNA-, RNA- and protein-binding (**Figure S11**) suggests that sexual differentiation relies on mechanisms spanning from regulation of gene expression to posttranslational protein modifications.

Based on the above indication, we annotated motifs related to regulatory protein activity in the genome using the Plant Transcription factor & Protein Kinase Identifier and Classifier (iTAK)[44]. Among all 22,186 protein sequences in the genome, 160 transcription factors, 157 transcriptional regulators and 344 protein kinases were annotated (**Figure 5**; **Tables S11-S12**). Remarkably, the two largest male-trait related modules were significantly enriched in regulatory gene functions. Module blue was significantly enriched in transcription factors (0.91%; multi-set interaction analysis, $p = 0.049$), transcriptional regulators (0.97%; $p = 0.010$) and protein kinases (1.97%; $p = 0.004$), while module coral2 was significantly enriched in transcription factors (1.14%; $p = 0.004$).

In comparison, the largest female trait-related modules green and greenyellow were strongly enriched in metabolic functions related to pigment synthesis and cell wall composition (**Figures S10-S11**). In combination with the comparatively large number of genes co-expressed in male trait-related modules, this analysis suggests that the male developmental pathway requires substantial reorganization of the transcriptome involving different regulatory pathways and epigenetic modifications, whereas female traits are correlated to smaller co-expression modules, which mainly have direct metabolic functions.

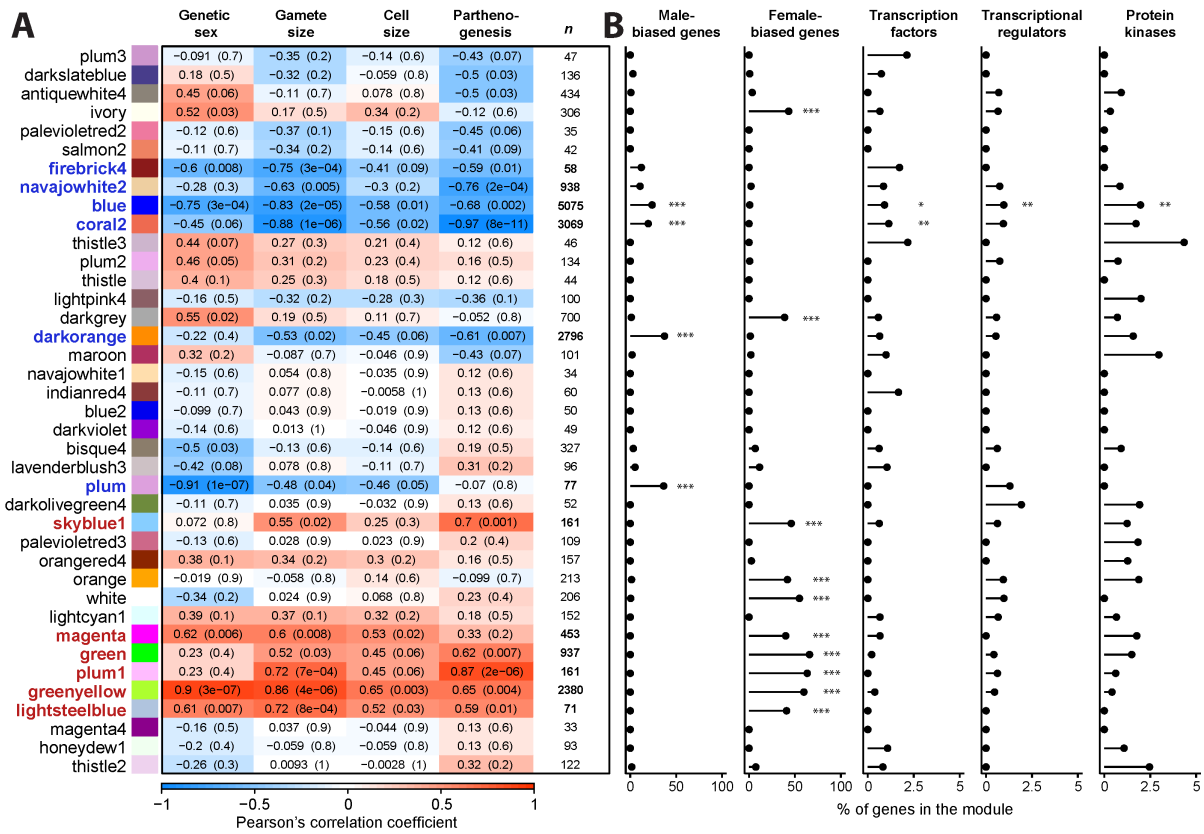

Figure 5 Properties of the 39 modules identified in the weighted gene co-expression network analysis of *Macrocystis pyrifera* wild type males, feminised males and wild type females. **(A)** Relation of module eigengenes to the assigned traits genetic sex, gamete size, gametophyte cell size, and parthenogenetic capacity. For each module and trait, Pearson's correlation coefficient (R) and *p*-value in parentheses are given. Twelve modules with R ≥ |0.6| and *p*-value ≤ 0.01 for at least one trait are highlighted in bold and blue (male trait-related) or red (female trait-related) font. Number of genes per module (*n*) is given on the right. **(B)** Prevalence of sex-biased genes and genes with regulatory function per module, with significant enrichment indicated in parentheses (***, $p < 0.0001$; **, $p < 0.001$; *, $p < 0.05$; multi-set intersection analyses).

Discussion

A female-like phenotype is the "ground state" of kelp gametophyte morphology

We show that the three male *M. pyrifera* variants Mpyr_13-4[24], Mpyr_fem1 and Mpyr_fem2 (this study), which were obtained in independent experiments from two distinct WT male gametophytes, present a similarly feminised phenotype. Despite being genetically males, they all share typical female features such as increased gametophyte cell and gamete dimensions, and parthenogenetic capacity. However, these feminised lines are uncapable of attracting and fusing with sperm, indicating they are not fully functional females. Moreover, the size of the gametophyte and gamete cells does not fully reproduce a female phenotype, suggesting they are partially sex-reversed, displaying an intermediate phenotype to WT males and females.

In the model brown alga *Ectocarpus*, the male (V) haplotype of the sex locus is dominant over the female (U) haplotype[45–47], implying that the dominant male developmental program triggered in the presence of a V-SDR would be superimposed on the background of a "default" female development[22,47]. Our *M. pyrifera* variants developed a sterile, partially sex-reversed phenotype, despite the presence of the male V-SDR and the absence of the female U-SDR. The fact that the transcriptome of the variants was significantly enriched in FBGs demonstrates that these are not

under direct control of the female sex locus, but rather that their expression may be repressed in WT male gametophytes, likely by the male master sex determining gene MIN. Therefore, we conclude that this feminised phenotype resembles a developmental "ground state" of gametophyte morphology, which is normally overridden in the presence of a male V-SDR, or complemented by the presence of a U-SDR to form a fully functional female.

Male development requires large-scale transcriptome reorganisation

In the WGCNA, more than half of all annotated genes in the genome were clustered into modules which were significantly correlated with male traits, whereas the significantly female trait-related modules covered less than 20% of the whole transcriptome. In addition, the two largest male trait-related modules were significantly enriched in genes with regulatory functions (*i.e.*, transcription factors, transcriptional regulators, protein kinases). In combination with the enrichment of GO terms related to regulatory functions in male trait-related modules, it appears that male development requires substantial restructuring of the cellular machinery involving mechanisms from gene expression regulation to posttranslational modifications, in comparison to the female developmental program, which targets metabolic processes more directly.

Interestingly, male trait-related co-expression modules were significantly enriched in GO terms related to chromatin structure and epigenetic histone marks. Histone modifications play a major role in the life cycle control of brown algae[47,48]. In the model *Ectocarpus*, 37% of SBGs were associated with differential histone marks between males and females[49]. Specifically, genes involved in male-specific development were mostly enriched in activation-associated marks in *Ectocarpus* males compared to females[49], suggesting a link between chromatin and activation of the male developmental program. It is likely that chromatin and epigenetic remodelling play a similar role in the sexual differentiation of kelp gametophytes, considering the stronger association of these processes with male rather than with female development, and the large-scale transcriptomic reorganisation we observed in association with male trait expression.

Our screens identified three genetically male *M. pyrifera* strains with a feminised phenotype, but no variant females with masculinized phenotypes were detected in parallel experiments. This observation supports the hypothesis that a male developmental program is superimposed on a female ground state, which would also be consistent with the presence of a master male-determinant gene. Transitions from male to female sex may therefore be more likely than the reverse in brown algae, potentially due to the central role of the master male sex determining gene *MIN* (and potential auxiliary sex-linked genes) which coordinate male development and the associated transcriptomic changes[25,47].

Increased turnover and faster evolution of male-biased genes

Our analysis revealed that MBG expression was largely species-specific, whereas female bias was more conserved across five different brown algal species. This observation indicates a higher turnover of expression in MBGs compared to FBGs and is coherent with recent reports in other brown algae with U/V systems[37], but also with animals and plants[50–52]. It is possible that sexual selection, acting mainly on males, is driving the evolution of MBG expression patterns. Remarkably, MBGs of brown algae with XX/XY systems in the order Fucales do not experience high turnover rates, but instead reveal remarkable conservation of bias and expression levels[53]. It is possible that the young age of the XX/XY system of the Fucales (65 Mya)[28,54], compared to the very old U/V system (> 450 Mya)[28,54], underlies these differences.

Moreover, *M. pyrifera* male-biased genes displayed accelerated rates of coding sequence evolution compared with female-biased or unbiased genes. A similar pattern was observed in *Saccorhiza polyschides* and *Sphacelaria rigidula*, which display oogamy and anisogamy, respectively, but not in the oogamous *Desmarestia herbacea*[37]. Thus, it appears that patterns of sequence evolution in genes involved in male versus female development vary significantly across species. It is possible that this species-specific pattern of gene evolution reflects positive selection pressures that drive the high turnover of genes involved in sex bias across brown algae, the diversity of gamete dimorphism and types of life cycles[20]. Note that increased evolutionary rates of MBGs have been largely documented in animals (reviewed by Grath & Parsch[55]) while similar patterns have not been found in plants[52,56,57].

In summary, the results of this analysis indicate that genes involved in male developmental patterns in giant kelp are fast evolving, whereas female genes evolve slowly. Therefore, it appears that the female developmental program is more conserved and involves more pleiotropic gene expression, whereas dominant, specific, and less conserved gene regulatory networks are activated during male development.

Role of the SDR in male and female developmental programs

A conspicuous trend of down-regulation of male SDR genes emerged in the feminised variants. In particular, this involved a gene encoding for a transmembrane protein and the male master sex determining gene Mp_HMG[22,25]. Both genes belong to an ancestral set of genes that have been consistently male-linked during brown algal evolution[26,28]. Additionally, Mp_13-001410, which was recently integrated into the SDR of kelps[26], may have taken on a role in male sexual differentiation in the kelps, as implied by its significant down-regulation across feminised variants. The repression of several male SDR genes is thus associated with the loss of the male phenotype. Therefore, it is possible that the role of MIN as master sex determinant may be complemented by other auxiliary sex-differentiation factors encoded by the male SDR.

Interestingly, none of the sex linked genes exhibited coding sequence mutations, so that the repression of male SDR genes described here imay be caused by autosomal factors or epigenetic regulators of male development, acting upstream of the SDR and controling both the activation of male-linked (V-SDR) genes and the repression of the feminized background. Therefore, (epi)genetic variation up- or downstream of the sex-determining genes may disrupt sexual differentiation even if the sex-determining genes themselves are not directly affected.

We identified a set of 24 genes which seem to be crucial for a fully functional female phenotype. Two of those genes have been shown to be located on the female SDR[26], but the high number of genes within this set with orthologs on the *Ectocarpus* sex chromosome suggests that more may have moved into the SDR of *M. pyrifera*. A full assembly of the kelp male and female SDR is currently not available and would be required to further explore this idea. Interestingly, the gametolog of the male-linked Mp_13-001840, gene g33225 (ortholog to *Ectocarpus* gene Ec-sdr_f_000170) is part of the female-restricted set of genes, making both genes of this gametolog pair candidates for antagonistic sex-determining factors. Additionally, the gametolog of the male-linked Mp_13-001910, g35582, codes for a STE20 protein kinase and has previously been suggested as central to female development in *M. pyrifera*[24] and across brown algae[28]. Therefore, our analysis confirms that these genes are ancestral gametolog pairs in *M. pyrifera*[26], and provide evidence for their central role in phenotype differentiation of both sexes.

Conclusion

In summary, our experiments are consistent with a female-like phenotype being the "ground-state" of giant kelp gametophyte morphology (**Figure 6**). The initiation of the male developmental program requires the presence of a V-SDR that includes the master male sex determining gene Mp_HMG (male inducer *MIN*)[25] together with accessory V-SDR linked genes. The male V-SDR therefore operates by repressing the female-like ground state while activating the male developmental program. The female U-SDR is crucial to the production of functional eggs, with the expression of a core set of U-linked genes providing key functions to complement the ground state developmental program and producing a functional female.

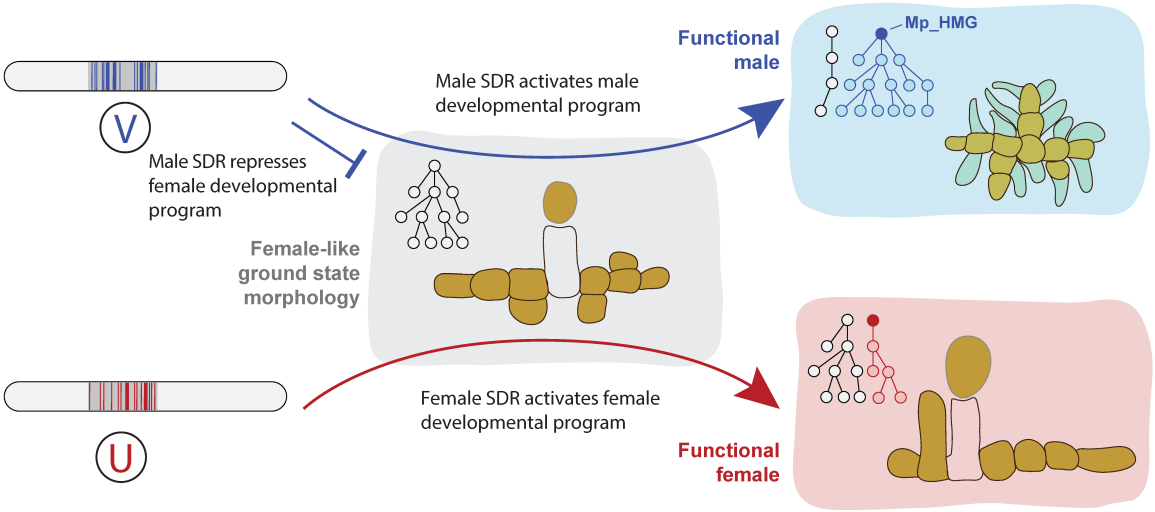

Figure 6 Conceptual model of sexual differentiation in *Macrocystis pyrifera*. In the presence of a male (V) sex-determining region (SDR), the gene expression network inducing the female-like, sterile ground state (grey) is repressed and large-scale transcriptomic networks are activated to produce a male phenotype (blue). In contrast, female-specific genes on the U-SDR complement the ground state developmental program to produce a functional female (red).

Methods

Biological material and phenotyping

Fertile sporophytes of the giant kelp *Macrocystis pyrifera* were collected at Curaco de Velez, Chile, in 2006. Meiospores were released and clonal cultures were established of two unialgal gametophyte isolates CVe13f female (CVe_female) and CVe30m male (CVe_male). Following colchicine treatment of the male gametophyte strain CVe30m as described by Müller et al.[24], the feminised variants Mpyr_fem1 and Mpyr_fem2 were isolated from a phenotypically heterogeneous gametophyte regenerate. Cultures were grown vegetatively under 25-30 µmol phot. m^{-2} s^{-1} red LED light[58] in a 14:10 h light:dark cycle at 14°C in 50% Provasoli-enriched seawater (PES[59] with iodine enrichment[60]). Genetic sex of the gametophytes was confirmed using PCR-based markers (**Table S1**; **Figure S2**; see Lipinska et al.[61]).

To conduct measurements of cell and gamete size, gametophyte tufts were ground carefully in an Eppendorf tube using a micropestle. Gametophyte fragments were sieved to obtain a fraction smaller than 100 µm and settled in 12 mL 100% PES. For measurements of vegetative cell size, gametophytes

were grown on coverslips within petri dishes filled with PES for two weeks under red light. Cells were stained with lactophenol blue on the coverslips, which were inverted onto a glass slide and images were taken at 400x magnification with a microscope camera (acA2440-75um, Basler, Ahrensburg, Germany) fitted to an inverted microscope (Axio Vert.A1, Zeiss, Jena, Germany). All measurements were conducted with ImageJ Fiji[62].

Fertilization of ground gametophyte fragments was induced after 2 days at reduced irradiance of 5-10 µmol photons m^{-2} s^{-1} white LED light in a 14:10 h light:dark cycle (aquaLUMix AMAZON-GROW, LEDaquaristik GmbH, Hövelhof, Germany) at 12°C to facilitate gametophyte recovery from grinding. To induce fertility, irradiance was raised to 20-30 µmol photons m^{-2} s^{-1}. After 7 days, dishes with Mpyr_fem1 were moved to 50-70 µmol m^{-2} s^{-1} as no fertility had been observed until then. Medium was changed and cultures were observed every 3-4 days. Once the cultures were undergoing gametogenesis, photos were taken to measure gamete size and experimental crosses were produced to determine whether gametes of the feminised strains were capable of syngamy. Significant differences between strains in cell and gamete size were analysed by non-parametric Kruskal-Wallis rank sum tests followed by pairwise Wilcoxon rank sum tests with false discovery rate (FDR) *p*-value adjustment[63].

For the ploidy analysis, small tufts of gametophytes (20-50 mg fresh weight) were patted dry and cut to fine fragments in 500 µL of nuclei isolation buffer[64], with addition of 0.5 µg/L Proteinase K, 5‰ SDS, 0.1 mM Tris HCl pH 8.0. Nuclei were strained through a 10 µm nylon mesh and stained using 1X SYBR Green I. After 10 min incubation, DNA content was measured in an Agilent NovoCyte Advanteon flow cytometer.

RNA extraction and sequencing

Colonies of wild type CVe_male and CVe_female cultures, and the feminized male variants Mpyr_fem1 and Mpyr_fem2 were fragmented using tweezers and cultivated each in four replicate petri dishes (⌀ 55 mm) filled with 12 mL 100% PES at fertility-inducing conditions (see above) for 7 days. At the time of collection, reproductive features were not yet visible (to be comparable with Müller et al.[24]). Four lentil-sized replicates (approx. 20 mg fresh weight) per strain were patted dry in tissue paper, snap-frozen in liquid nitrogen and stored at -80°C.

Frozen biomass was homogenized in 1.5 mL centrifuge tubes using a micropestle while preventing thawing of the sample by submerging the tube frequently in liquid nitrogen. Lysis was performed in 1 mL CTAB3 buffer (100 mM Tris-HCl pH 8.0; 1.4 M NaCl; 20 mM EDTA pH 8.0; 2% Plant RNA Isolation Aid [Invitrogen, Waltham, USA]; 2% cetyltrimethyl ammonium bromide; 1% β-mercaptoethanol) for 15 min at 45°C. The organic phase was separated twice using the same volume of 24:1 chloroform:isoamylalcohol and centrifuging at 10,000 g for 15 min at 4°C. The upper aqueous phase was collected and RNA was precipitated overnight at -20°C in a solution of 3 M LiCl and 1% β-mercaptoethanol. RNA was collected by centrifuging at 18,200 g for 60 min at 4°C and the supernatant was discarded. The RNA pellet was washed twice in 1 mL 80% ice-cold Ethanol, air-dried and eluted in 30 µL nuclease-free water. DNA was removed using TURBO DNase (Invitrogen, Waltham, USA) according to the manufacturer's instructions and 35 µL of the supernatant were treated with the RNA Clean & Concentrator Kit 5 (Zymo Research, Irvine, USA) using an adapted protocol (the RNA prep buffer step was performed twice; RNA was washed in 700 µL wash buffer four times) and RNA was eluted in 15 µL nuclease-free water. RNA purity was confirmed by spectrophotometry (BioSpectrometer, Eppendorf, Hamburg, Germany), concentrations were measured by fluorometry (Qubit 4, Invitrogen, Waltham, USA) and RNA size distribution was confirmed using capillary electrophoresis (Agilent 2100 Bioanalyzer, Agilent Technologies, Santa Clara, United States).

Sequencing libraries were prepared using a commercial kit (NEBNext Ultra II Directional RNA Library Prep with Sample Purification Beads, New England Biolabs, Ipswich, USA), and cDNA of three replicates per strain was sequenced as 150 bp (100 bp for Mpyr_CVe13f) paired end libraries on an Illumina NextSeq2000 at the Genome Core Facility at the MPI Tübingen Campus.

Transcriptome analysis

Additionally to the data produced in this experiment, we re-analysed an RNA-seq dataset including the colchicine-treated feminised male *M. pyrifera* gametophyte Mpyr_13-4 and the two wild types Cur6m male (Cur_male) and Cur4f female (Cur_female), which had been produced in an independent experiment using a different male gametophyte[24]. This yielded a dataset with three feminised variants, two wild type males and two wild type females from two independent experiments.

Read quality and adapter trimming, mapping and gene expression values were performed according to the pipeline by Perroud et al.[65], using gmap-gsnap version 2021-12-17[66] and subread version 2.0.3[67]. The *M. pyrifera* genome by Lipinska et al.[42] was used as reference and modified on the SDR contigs. Differential expression between samples within the two independent experiments was assessed using DeSeq2 version 1.38.2[36].

Transcript abundances were calculated as transcript per million (TPM) and normalized as log(TPM+1). For each gametophyte line, all genes with average TPM values > 5th percentile, excluding genes with null expression, were considered as expressed. The significance threshold for differentially expressed genes was considered at $\log_2$ fold-change ($\log_2$FC) > 1 and adjusted *p*-value (FDR) < 0.001. All genes differentially expressed between the respective female and male wild types per experiment (CVe_female vs. CVe_male; Cur_female vs. Cur_male) were considered sex-biased genes. Significant enrichment of sex-biased genes in the variants was assessed using multi-set intersection analyses (R package SuperExactTest)[38]. All analyses and figures were produced in R version 4.2.1[68].

Functional annotation of genome protein sequences against the NCBI non-redundant (NR) database was performed using Diamond[69] and only top hits were retained. Of 22186 annotated gene products, 19910 (89.74%) were functionally annotated. Annotation using the Kyoto Encyclopedia of Genes and Genomes (KEGG) covered 17.38% of genes. Gene ontology (GO) annotation had been performed previously using Blast2GO[24,70], and covered 10460 genes (47.15%). Gene ontology (GO) term enrichment within differentially expressed gene sets was analysed using topGO[71].

Weighted gene co-expression network analysis (WGCNA) was then conducted on the concatenated dataset using R package wgcna[43]. To account for baseline differences between the two experiments, batch effects were removed from the log(TPM+1) data using removeBatchEffect in R package limma[72]. A signed network was constructed using a biweight midcorrelation ("bicor"), a soft thresholding power of 18, and maximum portion of outliers of 0.05. Modules were constructed with a minimum size of 30 genes and were merged to a correlation threshold of 0.75. We correlated gene co-expression to the traits genetic sex (1=female, 0=male), mean gamete size, mean cell size, and parthenogenesis (1=present, 0=absent). Modules with strong Pearson's correlation ($|R| \geq 0.6$) and significance ($p \leq 0.01$) to one or several traits were identified for further analysis. Transcription factors, transcriptional regulators and protein kinases were annotated in the protein sequences of the genome using the online tool Plant Transcription factor & Protein Kinase Identifier and Classifier (iTAK)[44], and significance of enrichment was calculated by multi-set intersection analyses (SuperExactTest)[38].

RNA-seq variant analysis

Variant calling and filtering was performed according to Haas et al.[73] with GATK package version 4.2.6.1[74]. Lists of sequence variants were compared between strains to retain only variants specific to

WT males and feminised males. All sequence variations appearing only in one dataset (WT male vs. feminised male) were marked as potential candidates which were manually curated in JBrowse[39].

Gene orthology and evolutionary rates

We inferred gene orthology between the five brown algae species *M. pyrifera*, *Desmarestia herbacea*, *Saccorhiza polyschides*, *Sphacelaria rigidula* and *Sphaerotrichia firma* using Orthofinder[75], accessing the genomes published by Cossard et al.[37]. Significant enrichment of sex-biased genes among single-copy orthologous genes between species was calculated using multi-set intersection tests (SuperExactTest)[38].

To test for differences in rates of evolutionary divergence between different categories of sex-biased and unbiased genes, single-copy orthologous genes were identified for *M. pyrifera* and *Saccharina japonica*[76] using Orthofinder v2.5.2 with default parameters. Orthologous proteins between species pairs were aligned with MAFFT v.7.453[77], and the alignments were curated with Gblocks v.0.91[78] and back-translated to nucleotides using translatorX[79]. We used these nucleotide alignments as input for phylogenetic analysis by maximum likelihood (PAML4.9, CodeML) to infer pairwise dN/dS with the F3x4 model of codon frequencies. Differences in evolutionary rates were assessed with Mann-Whitney ranked tests after filtering out sequences saturated in synonymous mutations (dS > 3).

Data availability

The NGS datasets generated for this study are available at the NCBI BioProject PRJNA1072278. The additional dataset by Müller et al.[24] is available at NCBI BioProject PRJNA694578. The modified *M. pyrifera* reference genome and annotation files are available at https://doi.org/10.17617/3.G6SL3X.

Acknowledgments

We thank Dieter Müller for providing the strains used in this study, and Martin Gachenot for support in the ploidy analysis. We thank the BMBF-funded de.NBI Cloud within the German Network for Bioinformatics Infrastructure (de.NBI) (031A532B, 031A533A, 031A533B, 031A534A, 031A535A, 031A537A, 031A537B, 031A537C, 031A537D, 031A538A). Computations were also performed in the MPCDF Cobra supercomputer and the cluster of the Max Planck Campus in Tübingen, Germany. This work was supported by the MPG, the ERC (grant n. 864038 to SMC) the Moore Foundation (GBMF11489, SMC) and the Bettencourt-Schuller Foundation (SMC). JBR was supported by a Humboldt Research Fellowship for postdoctoral researchers from the Alexander von Humboldt Foundation.

Author contributions

DL: Investigation (lead); Formal analysis (lead); Visualization (lead), Writing – original draft (lead), Writing – review and editing (supporting).

RL, EA, MZ, OG, JBR: Investigation (equal); Methodology (supporting)

GC: Investigation (equal), Methodology (equal); Visualization (supporting)

FBH: Data curation (lead); Visualization (supporting)

SMC: Conceptualization (lead); Funding acquisition (lead); Methodology (equal); Project administration (lead); Visualization (supporting); Writing – review and editing (lead).

Bibliography

1. Parker, G.A., Baker, R.R., and Smith, V.G.F. (1972). The origin and evolution of gamete dimorphism and the male-female phenomenon. J. Theor. Biol. *36*, 529–553. 10.1016/0022-5193(72)90007-0.

2. Hanschen, E.R., Herron, M.D., Wiens, J.J., Nozaki, H., and Michod, R.E. (2018). Multicellularity drives the evolution of sexual traits. Am. Nat. *192*, E93–E105. 10.1086/698301.

3. Lehtonen, J., Parker, G.A., and Schärer, L. (2016). Why anisogamy drives ancestral sex roles. Evol. *70*, 1129–1135. 10.1111/evo.12926.

4. Bulmer, M.G., and Parker, G.A. (2002). The evolution of anisogamy: a game-theoretic approach. Proc. R. Soc. Lond. B *269*, 2381–2388. 10.1098/rspb.2002.2161.

5. Bachtrog, D. (2006). A dynamic view of sex chromosome evolution. Curr. Opin. Genet. Dev. *16*, 578–585. 10.1016/j.gde.2006.10.007.

6. Bachtrog, D., Kirkpatrick, M., Mank, J.E., McDaniel, S.F., Pires, J.C., Rice, W., and Valenzuela, N. (2011). Are all sex chromosomes created equal? Trends Genet. *27*, 350–357. 10.1016/j.tig.2011.05.005.

7. Mank, J.E. (2009). Sex chromosomes and the evolution of sexual dimorphism: lessons from the genome. Am. Nat. *173*, 141–150. 10.1086/595754.

8. Parsch, J., and Ellegren, H. (2013). The evolutionary causes and consequences of sex-biased gene expression. Nat. Rev. Genet. *14*, 83–87. 10.1038/nrg3376.

9. Charlesworth, D. (2019). Young sex chromosomes in plants and animals. New Phytol. *224*, 1095–1107. 10.1111/nph.16002.

10. Feng, G., Sanderson, B.J., Keefover-Ring, K., Liu, J., Ma, T., Yin, T., Smart, L.B., DiFazio, S.P., and Olson, M.S. (2020). Pathways to sex determination in plants: how many roads lead to Rome? Curr. Opin. Plant Biol. *54*, 61–68. 10.1016/j.pbi.2020.01.004.

11. Koopman, P., Gubbay, J., Vivian, N., Goodfellow, P., and Lovell-Badge, R. (1991). Male development of chromosomally female mice transgenic for *Sry*. Nature *351*, 117–121. 10.1038/351117a0.

12. Harkess, A., Zhou, J., Xu, C., Bowers, J.E., Van der Hulst, R., Ayyampalayam, S., Mercati, F., Riccardi, P., McKain, M.R., Kakrana, A., et al. (2017). The asparagus genome sheds light on the origin and evolution of a young Y chromosome. Nat. Commun. *8*, 1279. 10.1038/s41467-017-01064-8.

13. Müller, N.A., Kersten, B., Leite Montalvão, A.P., Mähler, N., Bernhardsson, C., Bräutigam, K., Carracedo Lorenzo, Z., Hoenicka, H., Kumar, V., Mader, M., et al. (2020). A single gene underlies the dynamic evolution of poplar sex determination. Nat. Plants *6*, 630–637. 10.1038/s41477-020-0672-9.

14. Kurtz, S., Lucas-Hahn, A., Schlegelberger, B., Göhring, G., Niemann, H., Mettenleiter, T.C., and Petersen, B. (2021). Knockout of the HMG domain of the porcine SRY gene causes sex reversal in gene-edited pigs. Proc. Natl. Acad. Sci. U.S.A. *118*, e2008743118. 10.1073/pnas.2008743118.

15. Sakashita, A., Wakai, T., Kawabata, Y., Nishimura, C., Sotomaru, Y., Alavattam, K.G., Namekawa, S.H., and Kono, T. (2019). XY oocytes of sex-reversed females with a *Sry* mutation deviate from

the normal developmental process beyond the mitotic stage. Biol. Reprod. *100*, 697–710. 10.1093/biolre/ioy214.

16. Nagahama, Y., Chakraborty, T., Paul-Prasanth, B., Ohta, K., and Nakamura, M. (2021). Sex determination, gonadal sex differentiation, and plasticity in vertebrate species. Physiol. Rev. *101*, 1237–1308. 10.1152/physrev.00044.2019.

17. Coelho, S.M., Gueno, J., Lipinska, A.P., Cock, J.M., and Umen, J.G. (2018). U/V chromosomes and haploid sexual systems. Trends Plant Sci. *23*, 794–807. 10.1016/j.tplants.2018.06.005.

18. Fruchard, C., and Marais, G.A.B. (2021). The evolution of sex determination in plants. In Evolutionary Developmental Biology, L. Nuño de la Rosa and G. B. Müller, eds. (Springer International Publishing), pp. 683–696. 10.1007/978-3-319-32979-6_168.

19. Cock, J.M., Sterck, L., Rouzé, P., Scornet, D., Allen, A.E., Amoutzias, G., Anthouard, V., Artiguenave, F., Aury, J.-M., Badger, J.H., et al. (2010). The *Ectocarpus* genome and the independent evolution of multicellularity in brown algae. Nature *465*, 617–621. 10.1038/nature09016.

20. Heesch, S., Serrano-Serrano, M., Barrera-Redondo, J., Luthringer, R., Peters, A.F., Destombe, C., Cock, J.M., Valero, M., Roze, D., Salamin, N., et al. (2021). Evolution of life cycles and reproductive traits: Insights from the brown algae. J. Evol. Biol. *34*, 992–1009. 10.1111/jeb.13880.

21. Luthringer, R., Cormier, A., Ahmed, S., Peters, A.F., Cock, J.M., and Coelho, S.M. (2014). Sexual dimorphism in the brown algae. Perspectives in Phycology *1*, 11–26. 10.1127/2198-011X/2014/0002.

22. Ahmed, S., Cock, J.M., Pessia, E., Luthringer, R., Cormier, A., Robuchon, M., Sterck, L., Peters, A.F., Dittami, S.M., Corre, E., et al. (2014). A haploid system of sex determination in the brown alga *Ectocarpus* sp. Current Biology *24*, 1945–1957. 10.1016/j.cub.2014.07.042.

23. Lipinska, A., Cormier, A., Luthringer, R., Peters, A.F., Corre, E., Gachon, C.M.M., Cock, J.M., and Coelho, S.M. (2015). Sexual dimorphism and the evolution of sex-biased gene expression in the brown alga *Ectocarpus*. Mol. Biol. Evol. *32*, 1581–1597. 10.1093/molbev/msv049.

24. Müller, D.G., Gaschet, E., Godfroy, O., Gueno, J., Cossard, G., Kunert, M., Peters, A.F., Westermeier, R., Boland, W., Cock, J.M., et al. (2021). A partially sex-reversed giant kelp sheds light into the mechanisms of sexual differentiation in a U/V sexual system. New Phytologist. 10.1111/nph.17582.

25. Luthringer, R., Raphalen, M., Guerra, C., Colin, S., Martinho, C., Zheng, M., Hoshino, M., Badis, Y., Lipinska, A.P., Haas, F.B., et al. Repeated co-option of HMG-box genes for sex determination in brown algae and animals. in press.

26. Lipinska, A.P., Toda, N.R.T., Heesch, S., Peters, A.F., Cock, J.M., and Coelho, S.M. (2017). Multiple gene movements into and out of haploid sex chromosomes. Genome Biol. *18*, 104. 10.1186/s13059-017-1201-7.

27. Zhang, L., Li, J., Wu, H., and Li, Y. (2019). Isolation and expression analysis of a candidate gametophyte sex determination gene (*SJHMG*) of kelp (*Saccharina japonica*). J. Phycol. *55*, 343–351. 10.1111/jpy.12821.

28. Barrera-Redondo, J., Lipinska, A.P., Liu, P., Dinatale, E., Cossard, G., Bogaert, K., Hoshino, M., Avia, K., Leiria, G., Avdievich, E., et al. (2024). Origin and evolutionary trajectories of brown algal sex chromosomes. Preprint at bioRxiv, 10.1101/2024.01.15.575685 10.1101/2024.01.15.575685.

29. Kain, J.M. (1979). A view of the genus *Laminaria*. Oceanogr. Mar. Biol. Ann. Rev. *17*, 101–161.

30. Klochkova, T.A., Motomura, T., Nagasato, C., Klimova, A.V., and Kim, G.H. (2019). The role of egg flagella in the settlement and development of zygotes in two *Saccharina* species. Phycologia *58*, 145–153. 10.1080/00318884.2018.1528804.

31. Hollenberg, G.J. (1939). Culture studies of marine algae. I. *Eisenia arborea*. Am. J. Bot. *26*, 34–41. 10.2307/2436508.

32. Maier, I., Hertweck, C., and Boland, W. (2001). Stereochemical specificity of lamoxirene, the sperm-releasing pheromone in kelp (Laminariales, Phaeophyceae). Biol. Bull. *201*, 121–125. 10.2307/1543327.

33. Lewis, R.J., and Neushul, M. (1994). Northern and southern hemisphere hybrids of *Macrocystis* (Phaeophyceae). J. Phycol. *30*, 346–353. 10.1111/j.0022-3646.1994.00346.x.

34. Gall, E.A., Asensi, A., Marie, D., and Kloareg, B. (1996). Parthenogenesis and apospory in the Laminariales: A flow cytometry analysis. Eur. J. Phycol. *31*, 369–380. 10.1080/09670269600651601.

35. Westermeier, R., Patiño, D., and Müller, D.G. (2007). Sexual compatibility and hybrid formation between the giant kelp species Macrocystis pyrifera and M. integrifolia (Laminariales, Phaeophyceae) in Chile. J. Appl. Phycol. *19*, 215–221. 10.1007/s10811-006-9126-7.

36. Love, M.I., Huber, W., and Anders, S. (2014). Moderated estimation of fold change and dispersion for RNA-seq data with DESeq2. Preprint at bioRxiv, 10.1101/002832 10.1101/002832.

37. Cossard, G.G., Godfroy, O., Nehr, Z., Cruaud, C., Cock, J.M., Lipinska, A.P., and Coelho, S.M. (2022). Selection drives convergent gene expression changes during transitions to co-sexuality in haploid sexual systems. Nat. Ecol. Evol. *6*, 579–589. 10.1038/s41559-022-01692-4.

38. Wang, M., Zhao, Y., and Zhang, B. (2015). Efficient test and visualization of multi-set intersections. Sci. Rep. *5*, 16923. 10.1038/srep16923.

39. Diesh, C., Stevens, G.J., Xie, P., De Jesus Martinez, T., Hershberg, E.A., Leung, A., Guo, E., Dider, S., Zhang, J., Bridge, C., et al. (2023). JBrowse 2: a modular genome browser with views of synteny and structural variation. Genome Biol. *24*, 74. 10.1186/s13059-023-02914-z.

40. Diesel, J., Molano, G., Montecinos, G.J., DeWeese, K., Calhoun, S., Kuo, A., Lipzen, A., Salamov, A., Grigoriev, I.V., Reed, D.C., et al. (2023). A scaffolded and annotated reference genome of giant kelp (*Macrocystis pyrifera*). BMC Genom. *24*, 543. 10.1186/s12864-023-09658-x.

41. Sterck, L., Billiau, K., Abeel, T., Rouzé, P., and Van de Peer, Y. (2012). ORCAE: online resource for community annotation of eukaryotes. Nat. Methods *9*, 1041–1041. 10.1038/nmeth.2242.

42. Lipinska, A.P., Serrano-Serrano, M.L., Cormier, A., Peters, A.F., Kogame, K., Cock, J.M., and Coelho, S.M. (2019). Rapid turnover of life-cycle-related genes in the brown algae. Genome Biol. *20*, 35. 10.1186/s13059-019-1630-6.

43. Langfelder, P., and Horvath, S. (2008). WGCNA: an R package for weighted correlation network analysis. BMC Bioinform. *9*, 559. 10.1186/1471-2105-9-559.

44. Zheng, Y., Jiao, C., Sun, H., Rosli, H.G., Pombo, M.A., Zhang, P., Banf, M., Dai, X., Martin, G.B., Giovannoni, J.J., et al. (2016). iTAK: a program for genome-wide prediction and classification of plant transcription factors, transcriptional regulators, and protein kinases. Mol. Plant *9*, 1667–1670. 10.1016/j.molp.2016.09.014.

45. Coelho, S.M., Godfroy, O., Arun, A., Le Corguillé, G., Peters, A.F., and Cock, J.M. (2011). *OUROBOROS* is a master regulator of the gametophyte to sporophyte life cycle transition in the brown alga *Ectocarpus*. Proc. Natl. Acad. Sci. U. S. A. *108*, 11518–11523. 10.1073/pnas.1102274108.

46. Müller, D.G., Maier, I., Marie, D., and Westermeier, R. (2016). Nuclear DNA level and life cycle of kelps: Evidence for sex-specific polyteny in *Macrocystis* (Laminariales, Phaeophyceae). J. Phycol. *52*, 157–160. 10.1111/jpy.12380.

47. Vigneau, J., Martinho, C., Godfroy, O., Zheng, M., Haas, F.B., Borg, M., and Coelho, S.M. (2023). Sex chromosome dominance in a U/V sexual system. Preprint at bioRxiv, 10.1101/2023.12.28.573518 10.1101/2023.12.28.573518.

48. Vigneau, J., and Borg, M. (2021). The epigenetic origin of life history transitions in plants and algae. Plant Reprod. *34*, 267–285. 10.1007/s00497-021-00422-3.

49. Gueno, J., Borg, M., Bourdareau, S., Cossard, G., Godfroy, O., Lipinska, A., Tirichine, L., Cock, J.M., and Coelho, S.M. (2022). Chromatin landscape associated with sexual differentiation in a U/V sex determination system. Nucleic Acids Res. *50*, 3307–3322. 10.1093/nar/gkac145.

50. Hollis, B., Houle, D., Yan, Z., Kawecki, T.J., and Keller, L. (2014). Evolution under monogamy feminizes gene expression in *Drosophila melanogaster*. Nat. Commun. *5*, 3482. 10.1038/ncomms4482.

51. Harrison, P.W., Wright, A.E., Zimmer, F., Dean, R., Montgomery, S.H., Pointer, M.A., and Mank, J.E. (2015). Sexual selection drives evolution and rapid turnover of male gene expression. Proc. Natl. Acad. Sci. U.S.A. *112*, 4393–4398. 10.1073/pnas.1501339112.

52. Scharmann, M., Rebelo, A.G., and Pannell, J.R. (2021). High rates of evolution preceded shifts to sex-biased gene expression in *Leucadendron*, the most sexually dimorphic angiosperms. eLife *10*, e67485. 10.7554/eLife.67485.

53. Hatchett, W.J., Jueterbock, A.O., Kopp, M., Coyer, J.A., Coelho, S.M., Hoarau, G., and Lipinska, A.P. (2023). Evolutionary dynamics of sex-biased gene expression in a young XY system: insights from the brown alga genus *Fucus*. New Phytol. *238*, 422–437. 10.1111/nph.18710.

54. Choi, S.-W., Graf, L., Choi, J.W., Jo, J., Boo, G.H., Kawai, H., Choi, C.G., Xiao, S., Knoll, A.H., Andersen, R.A., et al. (2024). Ordovician origin and subsequent diversification of the brown algae. Curr. Biol., S0960982223017694. 10.1016/j.cub.2023.12.069.

55. Grath, S., and Parsch, J. (2016). Sex-biased gene expression. Annu. Rev. Genet. *50*, 29–44. 10.1146/annurev-genet-120215-035429.

56. Darolti, I., Wright, A.E., Pucholt, P., Berlin, S., and Mank, J.E. (2018). Slow evolution of sex-biased genes in the reproductive tissue of the dioecious plant *Salix viminalis*. Mol. Ecol. *27*, 694–708. 10.1111/mec.14466.

57. Cossard, G.G., Toups, M.A., and Pannell, J.R. (2019). Sexual dimorphism and rapid turnover in gene expression in pre-reproductive seedlings of a dioecious herb. Ann. Bot. *123*, 1119–1131. 10.1093/aob/mcy183.

58. Lüning, K., and Dring, M.J. (1975). Reproduction, growth and photosynthesis of gametophytes of *Laminaria saccharina* grown in blue and red light. Mar. Biol. *29*, 195–200. 10.1007/BF00391846.

59. Starr, R.C., and Zeikus, J.A. (1987). UTEX—The culture collection of algae at the University of Texas at Austin. J. Phycol. *23*, 1–47.

60. Tatewaki, M. (1966). Formation of a crustaceous sporophyte with unilocular sporangia in *Scytosiphon lomentaria*. Phycologia *6*, 62–66. 10.2216/i0031-8884-6-1-62.1.

61. Lipinska, A.P., Ahmed, S., Peters, A.F., Faugeron, S., Cock, J.M., and Coelho, S.M. (2015). Development of PCR-based markers to determine the sex of kelps. PLoS ONE *10*, e0140535. 10.1371/journal.pone.0140535.

62. Schindelin, J., Arganda-Carreras, I., Frise, E., Kaynig, V., Longair, M., Pietzsch, T., Preibisch, S., Rueden, C., Saalfeld, S., Schmid, B., et al. (2012). Fiji: an open-source platform for biological-image analysis. Nat. Methods *9*, 676–682. 10.1038/nmeth.2019.

63. Benjamini, Y., and Hochberg, Y. (1995). Controlling the false discovery rate: A practical and powerful approach to multiple testing. J. R. Stat. Soc. Series B Stat. Methodol. *57*, 289–300. 10.1111/j.2517-6161.1995.tb02031.x.

64. Marie, D., Simon, N., Guillou, L., Partensky, F., and Vaulot, D. (2000). DNA/RNA analysis of phytoplankton by flow cytometry. Curr. Protoc. Cytom. *11*. 10.1002/0471142956.cy1112s11.

65. Perroud, P., Haas, F.B., Hiss, M., Ullrich, K.K., Alboresi, A., Amirebrahimi, M., Barry, K., Bassi, R., Bonhomme, S., Chen, H., et al. (2018). The *Physcomitrella patens* gene atlas project: large-scale RNA-seq based expression data. Plant J. *95*, 168–182. 10.1111/tpj.13940.

66. Wu, T.D., and Nacu, S. (2010). Fast and SNP-tolerant detection of complex variants and splicing in short reads. Bioinform. *26*, 873–881. 10.1093/bioinformatics/btq057.

67. Liao, Y., Smyth, G.K., and Shi, W. (2013). The Subread aligner: fast, accurate and scalable read mapping by seed-and-vote. Nucleic Acids Res. *41*, e108–e108. 10.1093/nar/gkt214.

68. R Core Team (2022). R: A Language and Environment for Statistical Computing. (R Foundation for Statistical Computing).

69. Buchfink, B., Reuter, K., and Drost, H.-G. (2021). Sensitive protein alignments at tree-of-life scale using DIAMOND. Nat. Methods *18*, 366–368. 10.1038/s41592-021-01101-x.

70. Conesa, A., and Götz, S. (2008). Blast2GO: a comprehensive suite for functional analysis in plant genomics. Int. J. Plant Genomics *2008*, 1–12. 10.1155/2008/619832.

71. Alexa, A., and Rahnenfuhrer, J. (2023). topGO: enrichment analysis for gene ontology. Version 2.52.0 (Bioconductor version: Release (3.17)). 10.18129/B9.bioc.topGO 10.18129/B9.bioc.topGO.

72. Ritchie, M.E., Phipson, B., Wu, D., Hu, Y., Law, C.W., Shi, W., and Smyth, G.K. (2015). *limma* powers differential expression analyses for RNA-sequencing and microarray studies. Nucleic Acids Res. *43*, e47–e47. 10.1093/nar/gkv007.

73. Haas, F.B., Fernandez-Pozo, N., Meyberg, R., Perroud, P.-F., Göttig, M., Stingl, N., Saint-Marcoux, D., Langdale, J.A., and Rensing, S.A. (2020). Single nucleotide polymorphism charting of *P. patens* reveals accumulation of somatic mutations during *in vitro* culture on the scale of natural variation by selfing. Front. Plant Sci. *11*, 813. 10.3389/fpls.2020.00813.

74. McKenna, A., Hanna, M., Banks, E., Sivachenko, A., Cibulskis, K., Kernytsky, A., Garimella, K., Altshuler, D., Gabriel, S., Daly, M., et al. (2010). The Genome Analysis Toolkit: a MapReduce framework for analyzing next-generation DNA sequencing data. Genome Res. *20*, 1297–1303. 10.1101/gr.107524.110.

75. Emms, D.M., and Kelly, S. (2019). OrthoFinder: phylogenetic orthology inference for comparative genomics. Genome Biol. *20*, 238. 10.1186/s13059-019-1832-y.

76. Ye, N., Zhang, X., Miao, M., Fan, X., Zheng, Y., Xu, D., Wang, J., Zhou, L., Wang, D., Gao, Y., et al. (2015). *Saccharina* genomes provide novel insight into kelp biology. Nat Commun. *6*, 6986. 10.1038/ncomms7986.

77. Katoh, K., Rozewicki, J., and Yamada, K.D. (2019). MAFFT online service: multiple sequence alignment, interactive sequence choice and visualization. Brief. Bioinform. *20*, 1160–1166. 10.1093/bib/bbx108.

78. Castresana, J. (2000). Selection of conserved blocks from multiple alignments for their use in phylogenetic analysis. Mol. Biol. Evol. *17*, 540–552. 10.1093/oxfordjournals.molbev.a026334.

79. Abascal, F., Zardoya, R., and Telford, M.J. (2010). TranslatorX: multiple alignment of nucleotide sequences guided by amino acid translations. Nucleid Acids Res. *38*, W7–W13. 10.1093/nar/gkq291.

Supplementary Figures

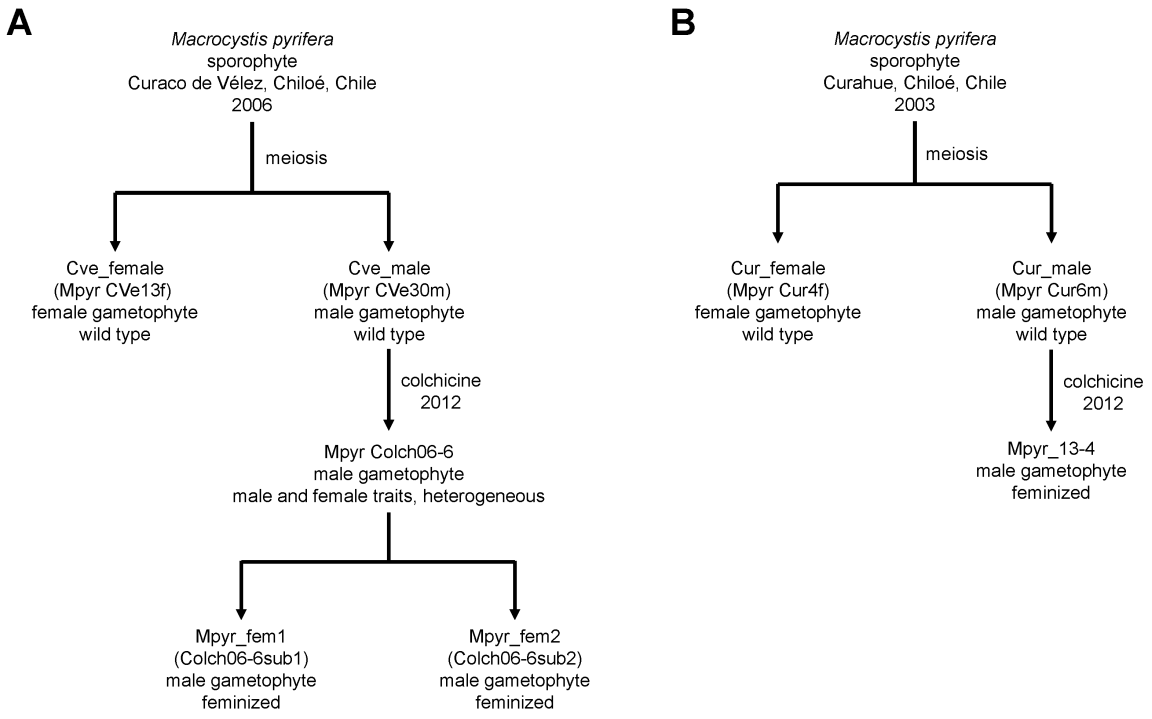

Figure S1 Pedigree of the *Macrocystis pyrifera* strains described **(A)** in this study and **(B)** in Müller et al.[24].

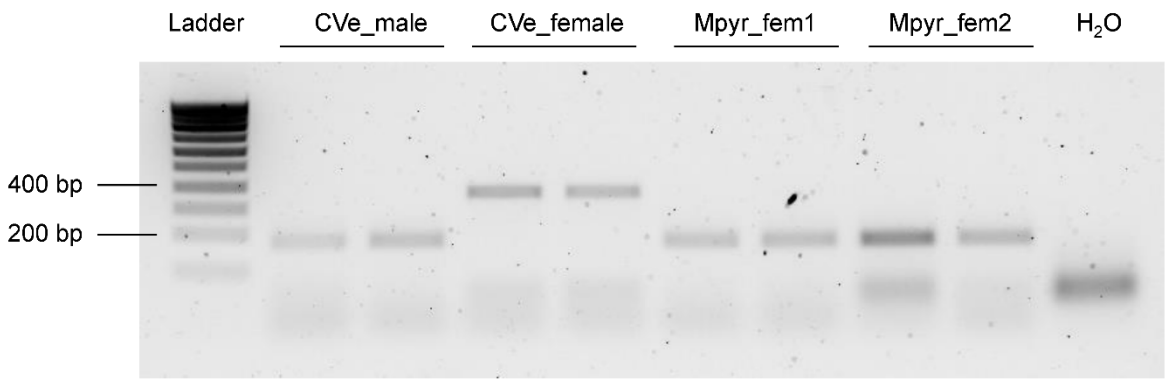

Figure S2 Gel electrophoresis pattern of PCR products of *Macrocysis pyrifera* gametophyte strains CVe_male (wild type male), CVe_female (wild type female), and Mpyr_fem1 and Mpyr_fem2 (feminised males). PCR products were run on a 1.8% Agarose gel for 20 min at 120 V. The target sequence of male marker Mac13.1750.1 (F, TTTCAGGTACGACGTGTTGG; R, CAATTCCGTCCAAGTCGTTT) amplifies at 180 bp, that of female marker Mp68_58ex3.4 (F, GTTGGTATAACGGCGTTGGA; R, CACCTCCTTAAAGTTGCGGC) amplifies at 350 bp. PCRs were conducted with both markers present in each reaction; for details see Table S1.

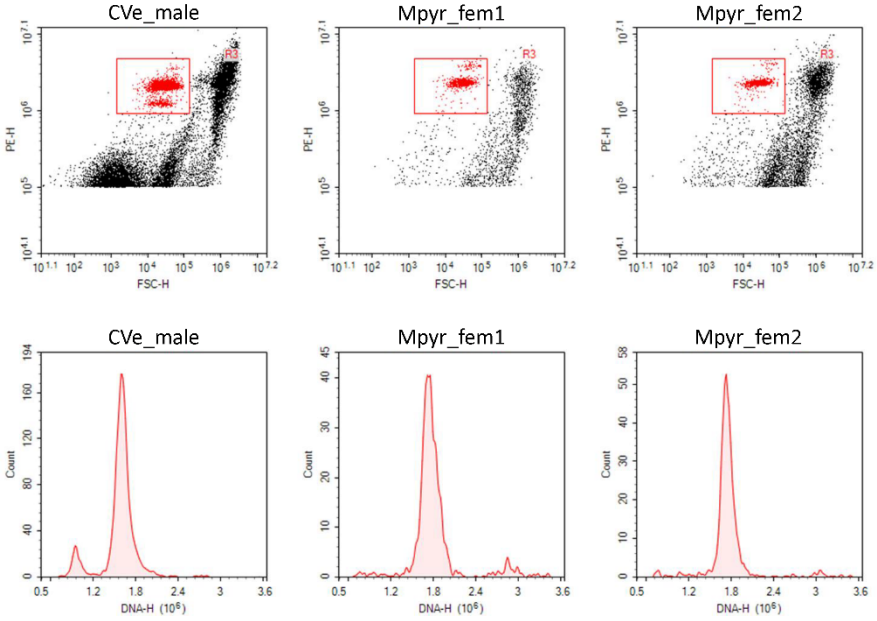

Figure S3 Results of flow cytometry analysis to estimate DNA content of *Macrocystis pyrifera* gametophyte strains CVe_male (wild type male), Mpyr_fem1 and Mpyr_fem2 (feminised male variants). Plots in the top row show populations of nuclei grouped by DNA content in scatterplots. Bottom row shows density plots of fluorescence signals as a proxy for DNA content.

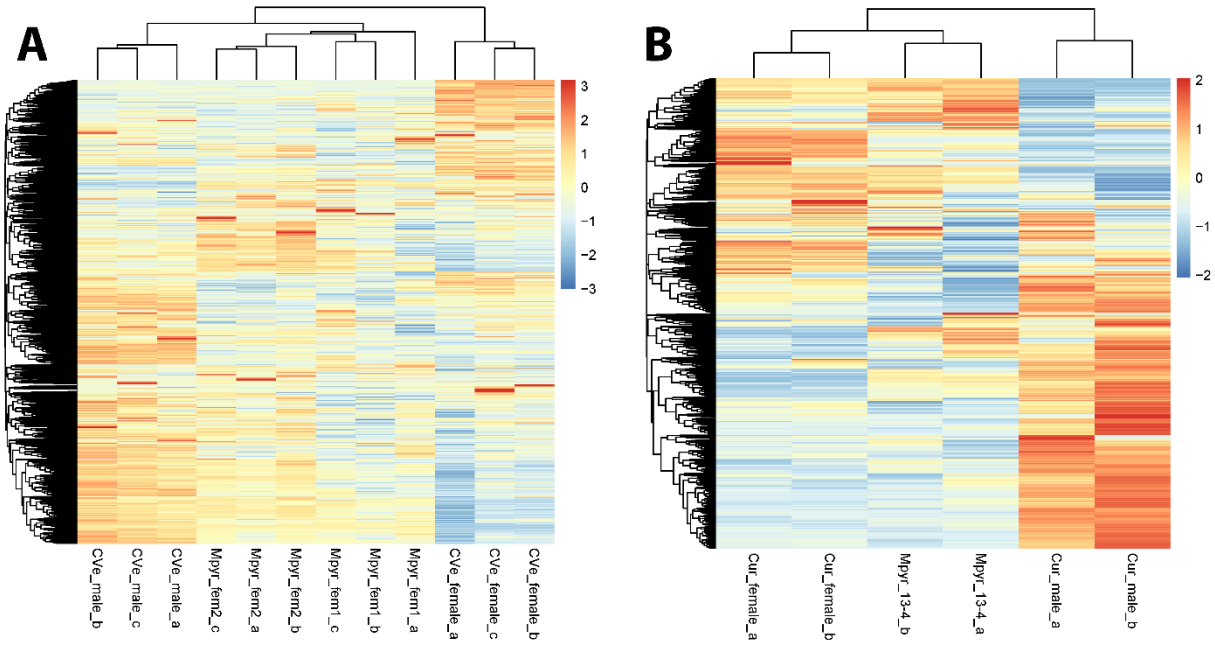

Figure S4 Global gene expression heatmap and hierarchical clustering based on z-score normalized log(TPM+1) expression values of *Macrocystis pyrifera* male wild types (CVe_male, Cur_male), feminised male variants (Mpyr_fem1, Mpyr_fem2, Mpyr_13-4) and female wild types (CVe_female, Cur_female) for two different experiments (**A**, this study; **B**, Müller et al.[24]).

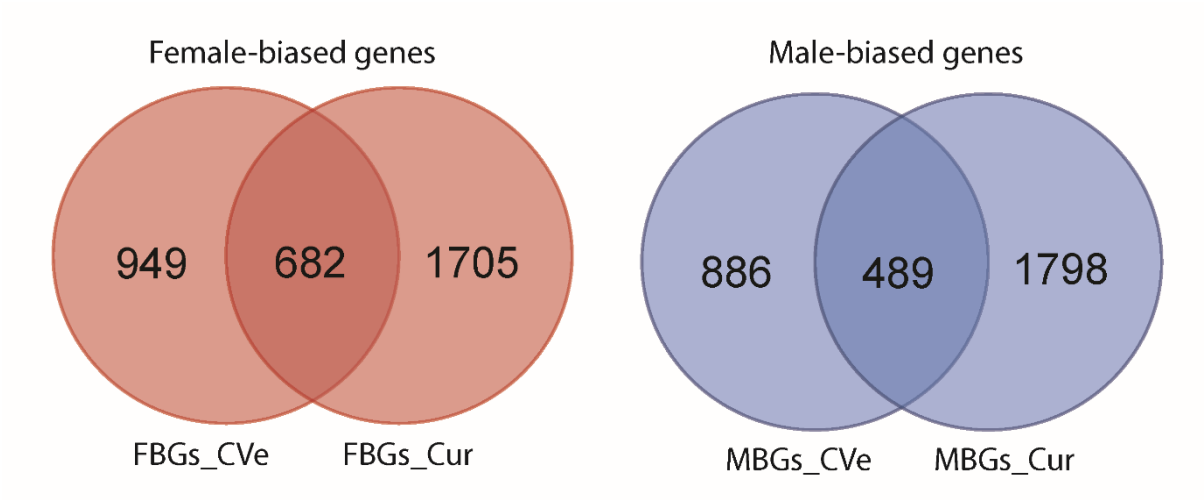

Figure S5 Venn diagrams depicting the number of shared sex-biased genes between the *Macrocystis pyrifera* populations CVe and Cur based on differentially expressed genes between wild type females and males.

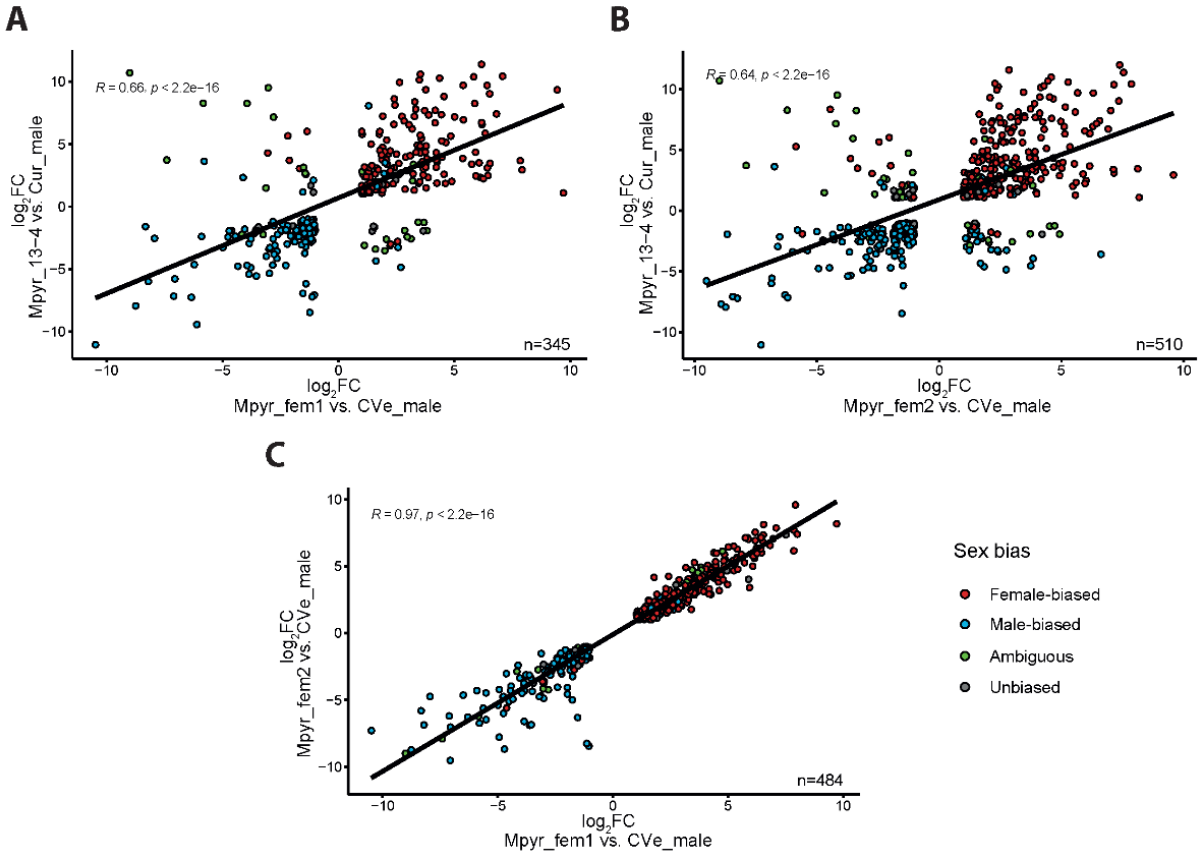

Figure S6 Correlation of $\log_2$FoldChange ($\log_2$FC) between comparisons for differentially expressed genes occurring in two comparisons (co_DEGs) of feminised variants and male wild types of *Macrocystis pyrifera*. Co-DEGs between **(A)** Mpyr_fem1 and Mpyr_13-4, **(B)** Mpyr_fem2 and Mpyr_13-4, **(C)** Mpyr_fem1 and Mpyr_fem2. Color indicates sex bias for each gene: red, female-biased in at least one family; blue, male-biased in at least one family; green, male-biased in one family and female-biased in the other (ambiguous); grey, no sex bias.

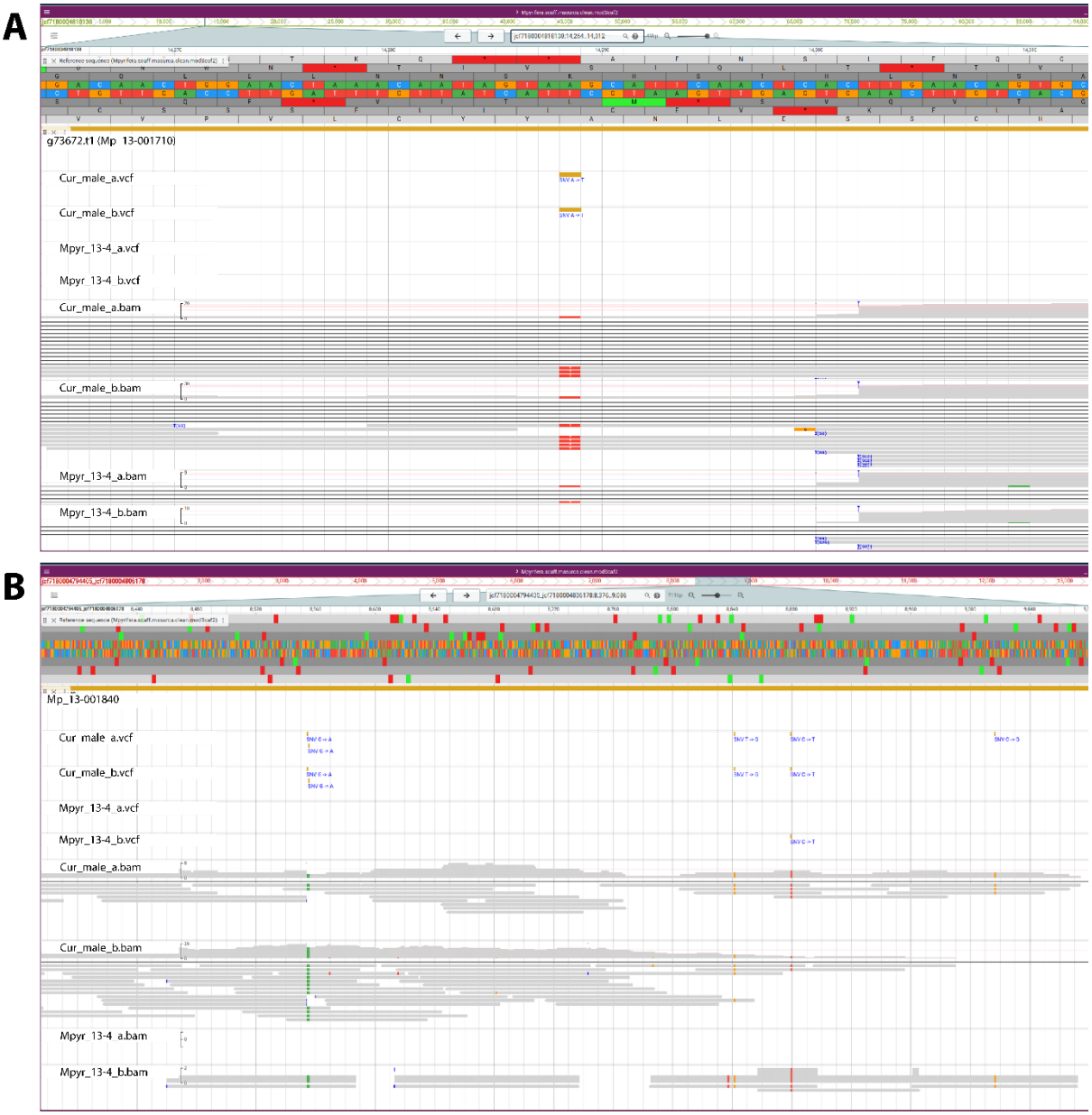

Figure S7. Visualisation of manual SNP assessment in a genome browser (JBrowse) representatively for genes **(A)** Mp_13-001710 and **(B)** Mp_13-001840 in the Cur population. Note that single nucleotide polymorphisms which were annotated only in the wild type Cur_male but not in the feminised variant Mpyr_13-4 (rows 1-4; *.vcf) were present in all samples including the feminised variant (rows 5-8; *.bam), but were not annotated in the variant due to low read coverage.

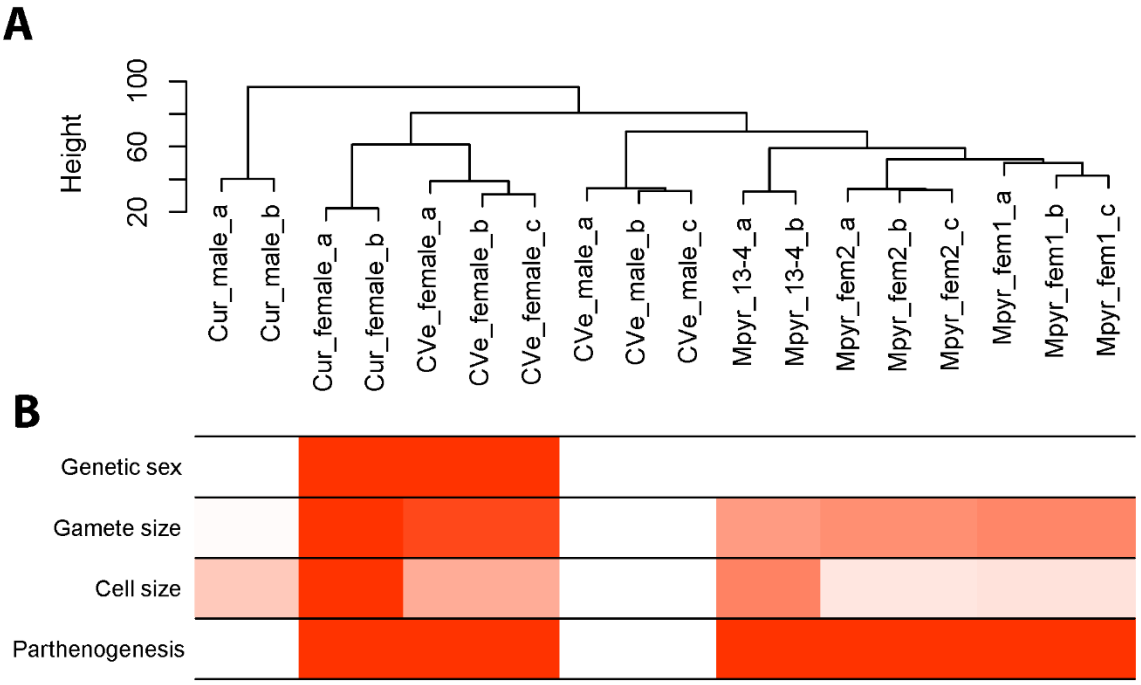

Figure S8. Sample clustering and trait association in the weighted gene co-expression network analysis on gene expression data of *Macrocystis pyrifera* male wild types (CVe_male, Cur_male), feminised male variants (Mpyr_fem1, Mpyr_fem2, Mpyr_13-4) and female wild types (CVe_female, Cur_female). **(A)** Clustering dendrogram of gene expression samples based on Euclidean distance. **(B)** Traits assigned to each sample visualised by colour intensity.

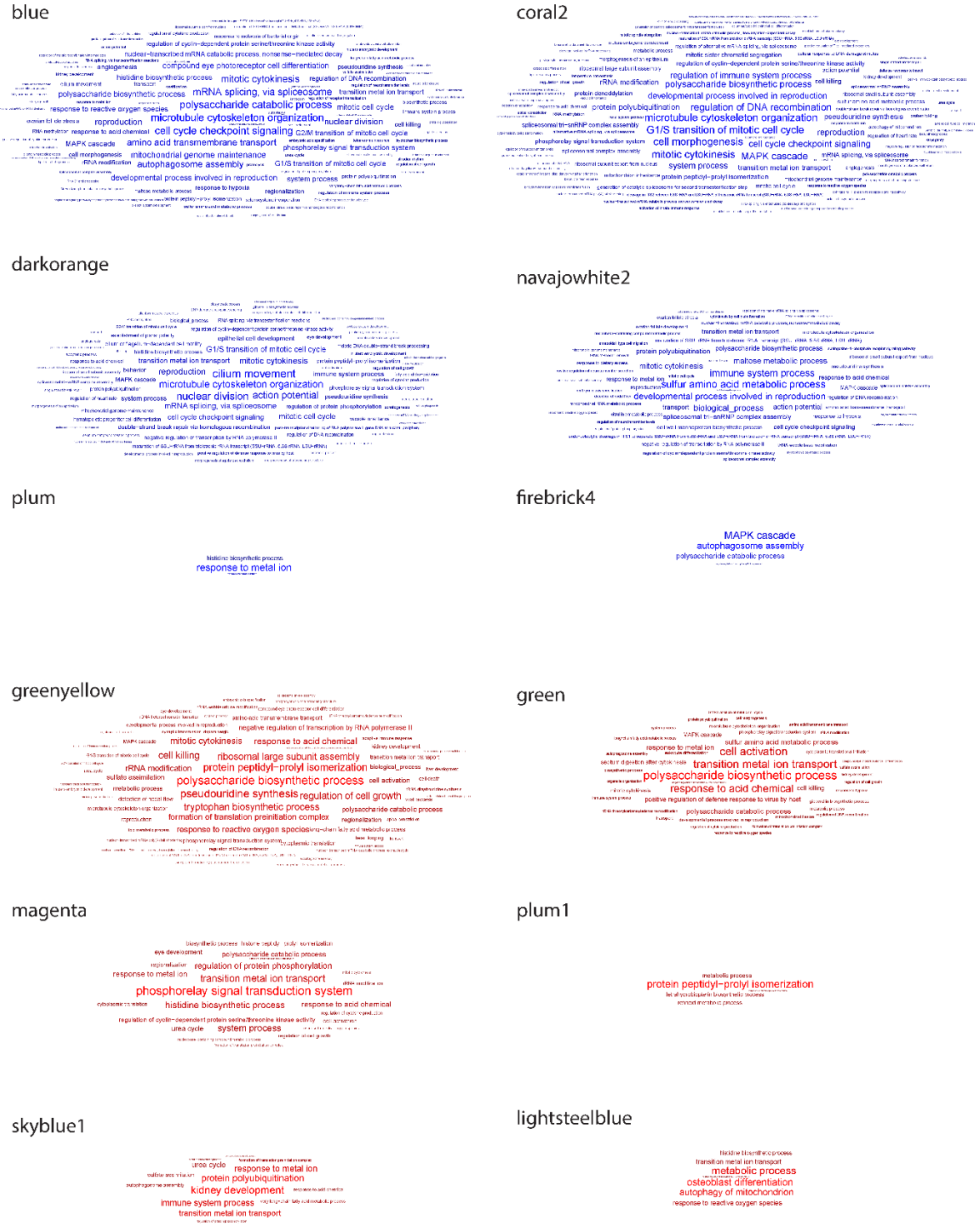

Figure S9. Significantly enriched gene ontology terms (biological process) in the twelve sex phenotype-related gene co-expression modules. Size of terms within each module correlates with -$\log_{10}$(*p*-value). Male trait-related modules are shown in blue, female trait-related modules in red.

blue

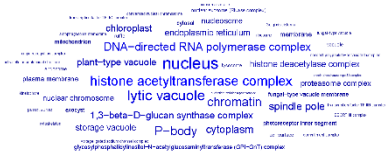

coral2

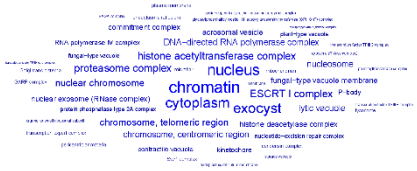

darkorange

navajowhite2

plum

firebrick4

greenyellow

green

magenta

plum1

skyblue1

lightsteelblue

Figure S10. Significantly enriched gene ontology terms (cellular component) in the twelve sex phenotype-related gene co-expression modules. Size of terms within each module correlates with -$\log_{10}$(*p*-value). Male trait-related modules are shown in blue, female trait-related modules in red.

blue

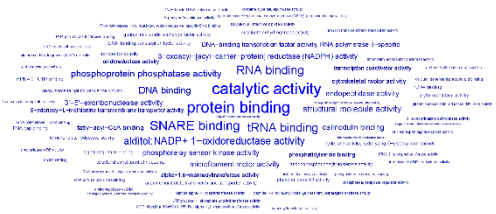

coral2

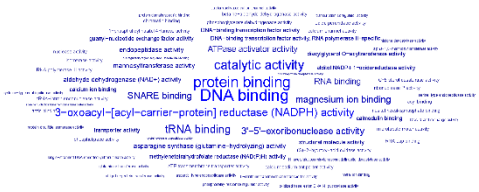

darkorange

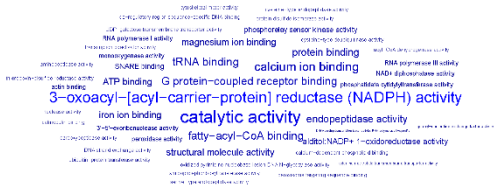

navajowhite2

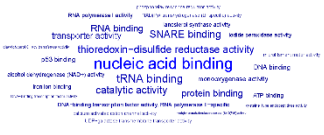

plum

firebrick4

greenyellow

green

magenta

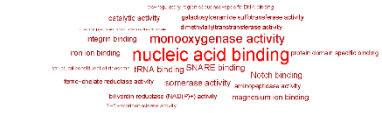

lightsteelblue

plum1

skyblue1

Figure S11. Significantly enriched gene ontology terms (molecular function) in the twelve sex phenotype-related gene co-expression modules. Size of terms within each module correlates with -$\log_{10}$(*p*-value). Male trait-related modules are shown in blue, female trait-related modules in red.

Supplementary Tables

Table S1 Sex-specific PCR markers used to confirm presence of the male V-chromosome and female U-chromosome of *Macrocystis pyrifera* gametophytes.

Table S2 List of *Macrocystis pyrifera* strains used and genome and transcriptome assembly statistics.

Table S3 Normalized read counts and DESeq2 results for *Macrocystis pyrifera* population CVe with variants Mpyr_fem1 and Mpyr_fem2.

Table S4 Normalized read counts and DESeq2 results for *Macrocystis pyrifera* population Cur with variant Mpyr_13-4[24].

Table S5 List of single-copy orthologs across five brown algae species *Macrocystis pyrifera*, *Sphacelaria rigidula*, *Sphaerotrichia firma*, *Desmarestia herbacea*, *Saccorhiza polyschides*[37].

Table S6 Functional gene annotation for significantly enriched gene ontology (GO) terms of feminisation shared by all three feminised variants of *Macrocystis pyrifera*.

Table S7 Functional gene annotation for significantly enriched gene ontology (GO) terms of de-masculinisation shared by all three feminised variants of *Macrocystis pyrifera*.

Table S8 List of all genes which are exclusively expressed in the wild type female of at least one population of *Macrocystis pyrifera* (CVe, Cur, shared), and indication of differential expression (DEG) vs. all genetical males within the population.

Table S9 Functional gene annotation for the core set of female-restricted genes of *Macrocystis pyrifera*.

Table S10 Alignment results of female-restricted genes (exclusively expressed in female wild types with significantly higher expression compared to male wild types and variants) of *Macrocystis pyrifera* gametophytes to reference genomes of *Macrocystis pyrifera* and *Ectocarpus* species 7. Shown are top hits for each query protein sequence. Sex chromosomes in the respective genome assemblies are highlighted in bold font.

Table S11 Functional gene annotation for all male trait-related modules (weighted gene co-expression network analysis) of *Macrocystis pyrifera*.

Table S12 Functional gene annotation for all female trait-related modules (weighted gene co-expression network analysis) of *Macrocystis pyrifera*.